UNIVERSITA' DEGLI STUDI DI PADOVA

Dipartimento di Ingegneria Industriale DII

Corso di Laurea Magistrale in Ingegneria Meccanica

Tesi di laurea

Experimental investigation on the use of extrusion cutting as material test

Relatori:

Prof. Stefania Bruschi

Prof. Leonardo De Chiffre

Correlatore:

Ing. Segalina Federico

Laureando: Antonio Landerghini *1178820*

Anno Accademico *2018/2019*

Abstarct

Questo lavoro presenta un'analisi dell' extrusion cutting come metodo per ottenere il flow stress del materiale sottoposto a condizioni estreme come elevata deformazione, velocità di deformazione e temperatura, che sono tipicamente ottenute in tornitura. In particolare, è stato testato l'extrusion cutting su ottone e rame puro utilizzando una nuova attrezzatura, progettata per eliminare i problemi di impostazione riscontrati in precedenti lavori. È stata condotta un'indagine sulla fattibilità dell'utilizzo dell'extrusion cutting al fine di avere un processo stabile con il rame, e per questo scopo sono stati modificati alcuni parametri di processo come l'angolo di spoglia frontale e la velocità di taglio. Inoltre, sono stati ottenuti molti dati sull'ottone ed è stato studiato il comportamento a diverse velocità di taglio, scoprendo che se il processo è stabile i dati sperimentali di diverse velocità di taglio, si mescoleranno perfettamente. In aggiunta, è stato esaminato lo studio teorico della temperatura raggiunta nel processo di extrusion cutting, riuscendo a ricavare un'equazione che considera anche la componente dispersiva di calore del pezzo.

List of Symbols

α Rake angle

β Friction angle

$\dot{\epsilon}$ Strain rate

γ Shear strain rate

ϵ Strain

η Contact length factor

γ Shear Strain

Λ Imposed chip compression factor

λ Chip compression factor

μ Coefficient of friction

φ Shear angle

σ Flow stress

τ Shear stress

F Friction force

Fc Cutting force

Fs Shear force

Ft Thrust force

Fx Dynamometer x-force

Fy Dynamometer y-force

z Dynamometer z-force

k Sher flow stress

L Length of contact tool-chip

N Force normal to tool rake face

p Specific cutting force

R Forces resultant

T Temperature

t Undeformed chip thickness

t’ Chip Thickness

v Cutting speed

v’ Chip speed

w Workpiece / chip width

D Diameter

Table of Contenents,

Chapter 1

1 Introduction to the project

In this chapter, the motivation of this master's project is presented along with the problem statement, goals, and research questions this thesis aims to answer. Moreover, the structure of this report and a brief description of the content aim to facilitate the reading and understanding of the thesis's work.

1.1 Backgroud

In the twentieth century, most of the comforts and services that are possible to find in everyday life in civilized countries, like any kind of transport (for example cars, ships, airplanes), water and energy transport systems, in agriculture and construction, they are all based on mechanical processes which, thanks to their technological progress, allow people to have increasingly efficient and affordable services for everyone. Many of these processes are based on metal processing, as the polymers and composites are still too technologically backward to replace metals. These processes range from foundry to plastic deformation such as extrusion, moulding, machining.

The first open source finite element simulators have appeared since the 1970s and companies have begun to use this method more and more frequently to become fundamental in many fields. In its original and still more widespread form, the finite element method is used to solve problems based on linear constitutive laws. Some more refined solutions allow to explore the behavior of materials even in the strongly non-linear field, hypothesizing plastic or visco-plastic behaviors. The advantages of finite element analysis consist in the possibility of dealing with the following problems:

• Define complex geometries (the heart and power of FEM methods)

• add different types of constraints for each analysis

• add different types of loading conditions

and succeed in obtaining different parameters as results (Fig.1).

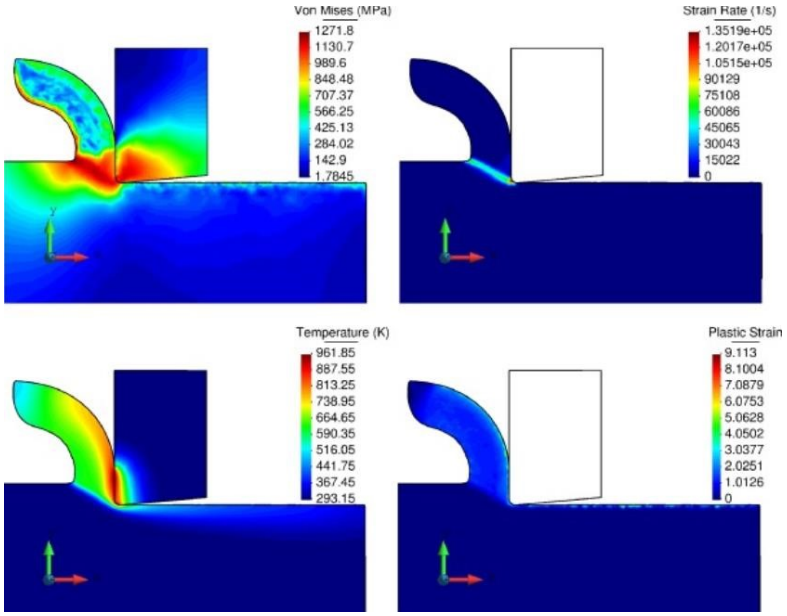

Figure 1: Example of fem simulation applied on metal cutting process [18].

If there is the possibility of simulating a process by changing and combining different parameters, and if this happens with a good agreement with reality, there will be the great advantage of reducing waste and costs, removing material where it is not needed and adding it where it is needed. This allows to design one mold without the need for post-modifications and in addition to finding the optimal processing parameters.

Most metalworking processes can be well simulated by FEM software, with the aforementioned advantages, and this is possible because the FEM software works with a numerical technique aimed at finding approximate solutions to problems described by partial differential equations reducing the latter to a system of algebraic equations.

Therefore, if in the software it is loaded the constitutive equation that describes the behaviour of the material in those determined conditions, the result will be exact. These equations will be obtained with controlled and reproducible laboratory tests. These equations are also used in numerical and analytical analysis and they are fundamental for the study of processes, especially at the theoretical level, and they are the base of the software FEM.

1.2 Motivation for the project

In the field of mechanical processing the most used processes such as foundry, plastic deformation, extrusion, molding, and drawing, are simulated with excellent correspondence to reality, allowing to choose the process parameters with almost 100% certainty that these parameters are optimum or as close to optimum as possible. Regarding the cutting (Fig. 2), the process simulation has still large gaps, as it is a very complex object of study to identify an equation capable of describing well the behavior of the material under the typical conditions of cutting.

This is because at the tip of the tool the strain, the strain rate, and the temperatures reached such high levels that it is impossible to reproduce them with tests for the characterization of the material.

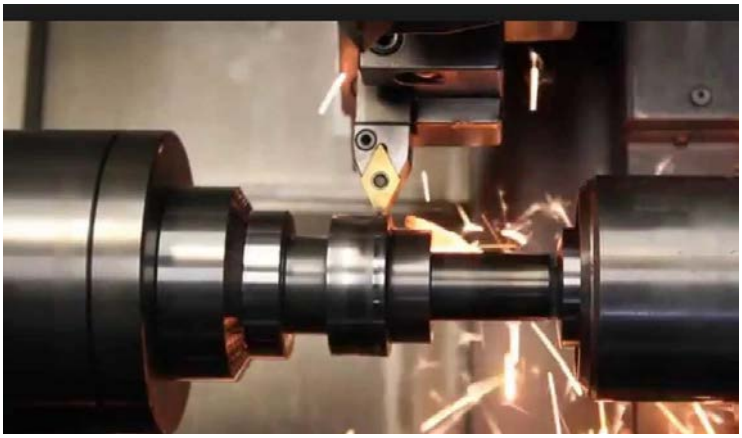

Figure 2: Turning process [19]

This entails the disadvantage of having large differences in simulation results with reality in terms of cutting time, tool wear and turned surface results.

The amount of money that revolves around machining is very high, and all companies that deal with this want to achieve lower process costs, to increase profits and competitiveness.

Independent Variables	Dependent Variables	Performance
▪ Machine ▪ Work ▪ Tool ▪ Cutting Fluid ▪ Cutting Data	▪ Contact ▪ Geometry ▪ Strains ▪ Speed ▪ Forces ▪ Temperatures ▪ Chip Form	▪ Product Quality ▪ Tool life ▪ Power and Forces ▪ Swarf evacuation

Table 1: Variables in metal cutting.

This can only be done by choosing the combination of optimal parameters (Tab.1) that until today has been based only on a few empirical formulas and on the experience of the operators.

Therefore, researches have been trying for many years to fill this gap for this important machining process.

1.3 Problem statement and goals

The traditional laboratory tests are still not able to replicate the physical characteristics of turning, above all the enormous strain rate, consider for example that the strain rate in turning has average values in the order of 10000 s^{-1}while the tests used so far have a strain rate of 3-4 orders of magnitude lower, in the order of maximum 1 or 2 s^{-1}.

To characterize the behavior of the material in turning conditions, it will be used in this work a test that is itself turning and in this way the data can be replicated with the same orders of magnitude.

This test is called extrusion cutting and by this test it could be derived a reliable constitutive equation of the material

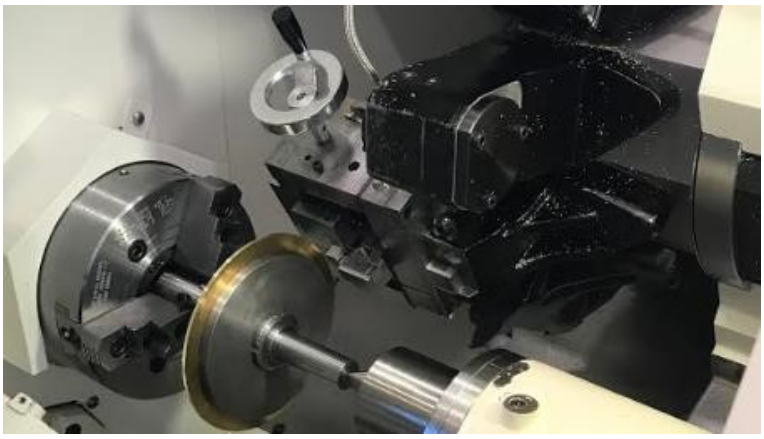

Figure 3: Extrusion Cutting equipment

1.4 Research questions

The following questions are those that have been defined to achieve the goals of this master's thesis. The aim of this work is to answer to the following research questions.

- Can extrusion cutting be considered a stable process?
- Does the theory of extrusion cutting describe the data obtained?
- Can extrusion cutting be applied to different materials?
- Can extrusion cutting be a method to find a constitutive equation that describes the behavior of the material in metal cutting?

1.5 Purpose

The purpose of this thesis is, first of all, to test whether the equipment for extrusion cutting works (Fig. 3), in the sense of verifying if it can be considered a stable and repeatable process since it is still in the experimental phase and it is constantly being modified.

After this, the equipment and the process will be tested for the application of new materials less theoretically prone compare to brass, such as copper and aluminium.

Then with the data collected, it will be derived a constitutive equation that describes the behavior of the material as faithfully as possible.

1.6 Introduction to FATI Group

Figure 4: FATI logo.

The company F.A.T.I. from Padua (Italy) manufactured the equipment used for the experimentation of extrusion cutting.

F.A.T.I. Srl is an engeneering and service company which has been working for more than 45 years with technical items for industry referring to metals and alloy steel, gaskets, plastic and rubber and precision mechanics.

F.A.T.I. gives customers also non-standard products; that is the reason why it became a leader in the production of gaskets and technical items for industry. Moreover, it has the know-how and the experience to suggest suitable and innovative materials to use for difficult applications.

They can work many kinds of materials for every single application, using a wide range of machineries including:

press for metal materials, CNC working centers, CNC and hand lathes, multi-axis pantographs, water cutting machine, self-adhesive machine, tumbling machine.

- It is organized in a quality system that allows:
  quality insurance that certifies company according to legislation, making everybody awareness of "quality policy"
- Quality control that involves all checking activities inside the company (controls when materials and items arrive, controls during the production, when production is finished and metrology) *Certified ISO 9001 : 2008*

This was not the first version of the equipment made by them, but a solid collaboration was established with the DTU, with the aim at achieving a concrete result that could revolutionize the world of metal cutting. Thus, the collaboration

continues until this thesis, with the latest updated, modified and improved version of the equipment.

Chapter 2

2 Literature review

In this chapter, a detailed literature review is provided for extrusion cutting process investigation. It has been tried to provide readers a general understanding of theoretical work and research that has been done in these areas. Moreover, it is tried to link the theoretical research with state of art of extrusion cutting.

2.1 Introduction into the process

Extrusion cutting is a metal cutting process most appropriately described as an orthogonal cutting process with an additional tool, termed the shoe, positioned as shown in figure 5.

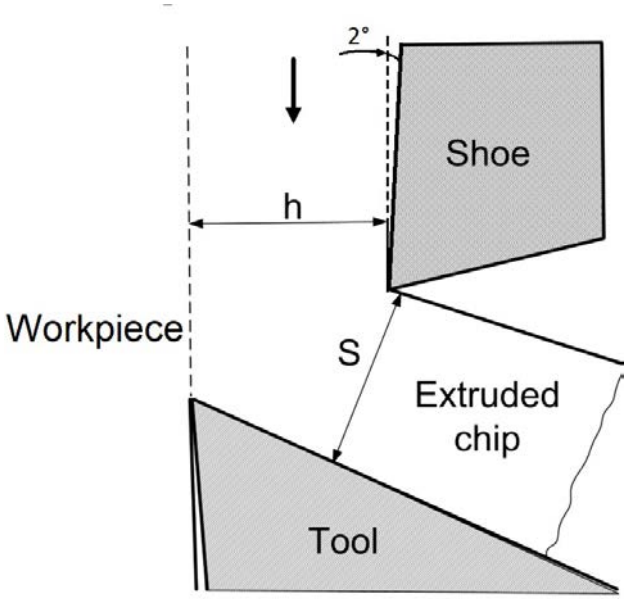

Figure 5: Sketch of extrusion cutting

The shoe serves to constrain the back surface of the chip, which would otherwise have been free to move, leaving the chip to be geometrically defined, a property not seen in normal orthogonal cutting, where the shape and curl of the chip are dependent on the properties of the material being cut and cutting condition see Table 1. Due to the chip constrained on both sides, the deformation of the chip is

determined solely by the shoe without respect to the material properties of the workpiece and rake angle.
The deformation in extrusion cutting that is imposed on the chip is termed the nominal chip compression ratio and it is defined by the tool-shoe gap,
while in the normal orthogonal cut without the shoe, the deformation that the chip undergoes is called the actual chip compression ratio.

Nominal chip compression ratio:

$$\Lambda = \frac{S}{h} \tag{2.1}$$

Where S is defined as the distance between shoe and tool, and h is defined as the shoe-tool offset, which corresponds to the feed imposed during processing (on the radius) it is easy to understand from figure 6.

The actual chip compression ratio:

$$\lambda = \frac{t\prime}{t} \tag{2.2}$$

Where t' denotes the thickness of the deformed chip, equivalent to S in equation 2.1, and t is equivalent to h, in equation 2.1 , in extrusion process, see figure 2.2.
The actual chip compression ratio is a characteristic parameter of orthogonal cutting. It depends on the characteristics of the material and the rake angle, for example for the MS63 brass turned with a 12° rake angle, the actual chip compression ratio is 2.9, while for the pure copper turned with a rake angle of 25° it is 8.

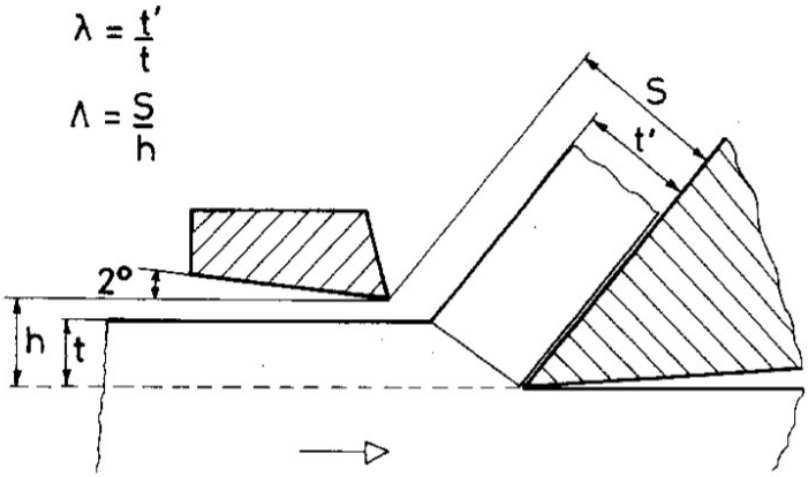

Figure 6: Relationship between machine feed shoe offset, chip thickness and tool-shoe gap. [2]

Therefore to note that if it is considered the case of the brass with imposed and constant feed, then t = h, it would have the coincidence of actual chip compression ratio and nominal chip compression ratio for 2.9 that is $\lambda = \Lambda = 2.9$ then from 2.9 to go down is possible to speak only of Λ (nominal chip compression ratio) because the extrusion begins.

2.1.1 Chip's quality

The chip surface changes after it gets narrow the shoe-tool gap more and more and the value of S will be reduced as it is shown in figure 7.

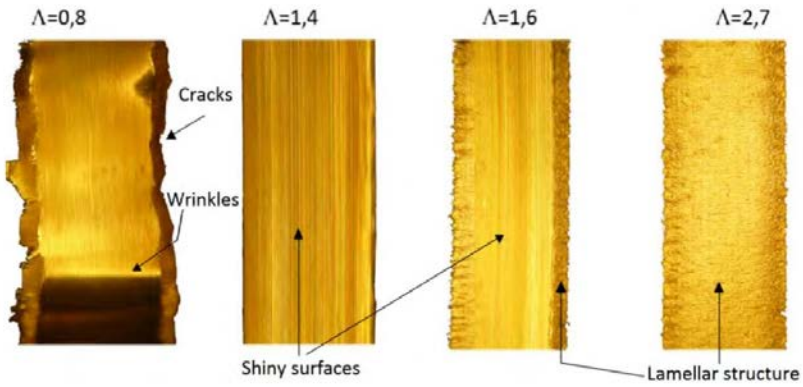

Figure 7: Extruded chips morphology for different tool-shoe gap. [3].

As shown in Figure 7, when the gap was large, the chip back surface was not constrained by the shoe. As the conditions were similar to normal cutting, a chip with a lamellar back surface were produced. Decreasing the gap, chip extrusion partially took place with a shiny surface in the middle of the chip and a rough morphology on the sides. Fully extruded chips were obtained for a chip compression factor imposed, Λ, of 1,4. Here, through all the chip width, the surface was shiny. Indeed, when the tool-shoe gap was around Λ=0,7, side cracks start being formed on the chip and wrinkles could be detected in the middle.
Another important factor, influencing the quality of the chips produced, is the alignment of the tool and shoe edges. If the setting of the chip thickness did not present any issue thanks to the employment of thickness gauges (Fig. 8b), a longitudinal curvature of the chip was obtained when the alignment between the edges was poor (Fig. 8a).

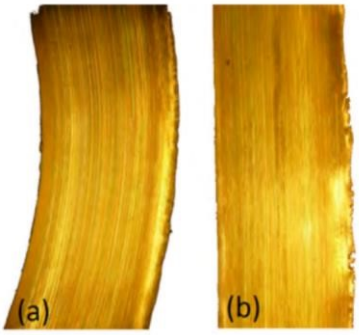

Figure 8: Extruded chips morphology for different tool-shoe edges alignment: (a)not aligned; (b)aligned. [3].

2.1.2 Hardness

The conventional brass chips are usually much harder than the work piece material, because of strain hardening behaviour at shear strain.
At contrary the extruded chips with extrusion cutting process, undergo lower shear strains, and, simultaneously, a thermal softening because of the heat confining effect by the shoe.
The hardness decreases as the shoe action becomes larger, around Λ=1.5 the hardness of extruded chip reaches the level of work material (Fig 9).
A further decrease in the gap led to hardness reduction and, for Λ=0,8, it was close to the level of the annealed work material (1 hour at 500°C).

The extruded chips have a lot of ductility left and, generally, they can not be fractured by repeated bending.

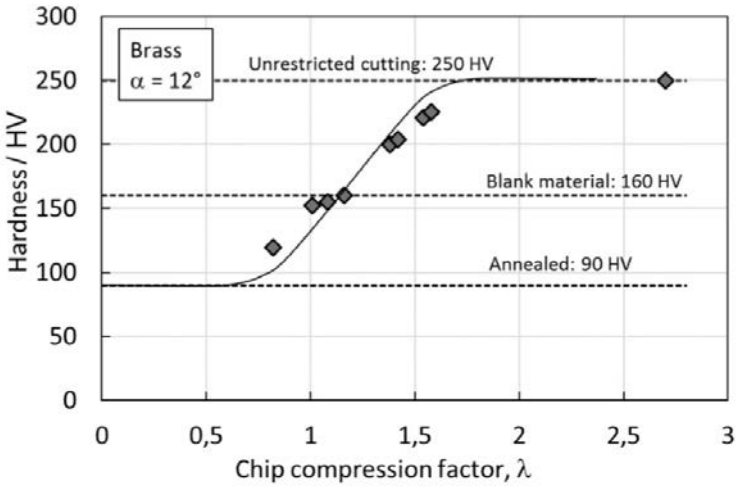

Figure 9: Hardness profile as function of chip compression factor. [3].

2.2 Applications of extrusion cutting

There are two main applications of this process:

- The production of strips and wires by means of a process that is expected to be more economical than other methods.
- The determination of flow stress data of metals being deformed under conditions of high strain, strain rate and temperature.

2.2.1 The production of strips and wires

The study “Extrusion Cutting of Brass Strips” by De Chiffre [2], it was concluded that the process can be considered stable, only if the following conditions are satisfied:

- The lathe and the set-up must be stiff enough and free from vibrations;
- Cutting tool and shoe must be sharp and, in particular, the shoe must be mounted at an entrance angle of about 2°;
- A feed of about one half of the shoe offset with respect to the tool should be adopted at the start of the cut, and then it must be increased rapidly to full feed;
- The experiments carried out on cast materials have shown that the work material must be homogeneous and totally free from pores;
- Finally, the tool-shoe gap has to be equal to approximately 1.5 times the feed, meaning that it should be employed a nominal chip compression of $\Lambda = 1.5$. This means that the quality of the chip produced depends strongly on the tool-shoe gap. A further decrease of the gap, though, leads to an increase of the material resistance to being extruded and, consequently, vibrations and folding of the strip take place and, eventually, side cracks start occurring in the strip.

The substantial advantage of extrusion cutting as a method for obtaining strips is the low manufacturing cost and the mechanical characteristics that the process give to the material's strips.
Large strain deformation of such an extrusion cutting chip formation may be expected to lead to a very fine microstructure, reinforced by a fine dispersion of precipitates that could result in chips with improved mechanical properties.
The role of large strain deformation in microstructure refinement was studied first by Embury and Fisher [8] and then Langford and Cohen [9]. Langford and Cohen [9] imposed large plastic strains in iron by repeated wire drawing and found the microstructure of the deformed iron wire to be composed of grains and dislocation substructures with sizes in the sub-micrometer range.

The use of similar, so-called severe plastic deformation (SPD) approaches to realize and study microstructure refinement is very interesting nowadays, and extrusion cutting is one of this [11],[12].
The extrusion cutting gives the material a plastic deformation such as to create a microcrystalline structure and moreover it happens with a strain rate so high as to induce a strain softening that reduces the hardness (Fig.10).

Figure 10: The ductility of a brass strip from extrusion cutting.

Hoshi and Shaw [10] succeed to produce wire with the cut-forming technique, which is a modified type of extrusion cutting, where the chip enter in the die.

2.2.2 Determination material's flow stress

Process as method to determinate flow stress data or better a constitutive equations under conditions of high strain, strain rate and temperature.

Constitutive equations:

Constitutive equations are mechanical equations of state that qualitatively and phenomenologically describe the reactions of mechanically loaded materials in dependence of the load and structural parameters.
they describe how the material responds to external stimuli.

With extrusion cutting it is possible to derive the flow stress or even better a constitutive equation that describes the material in the exceptionally extreme conditions that are found at the tip of the tool in turning. This is because the process of extrusion cutting works with almost the same conditions that the researchers are looking for. But at the same time it is a geometrically controlled process.

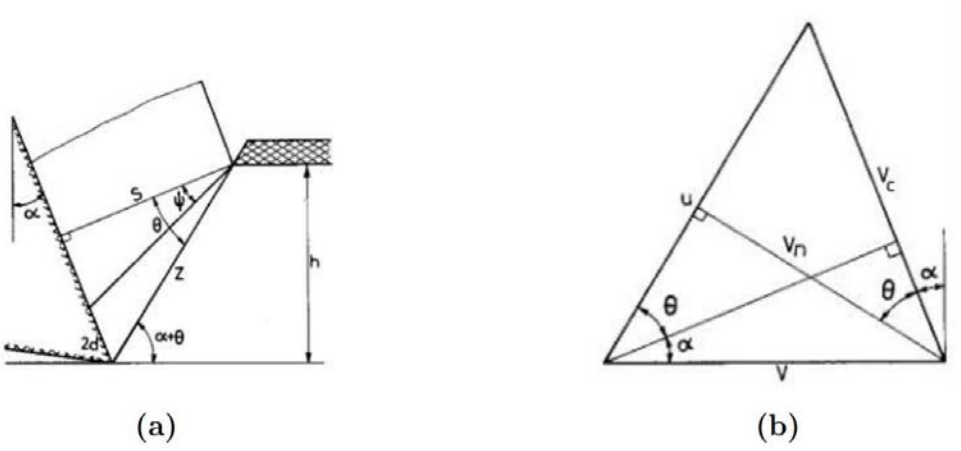

Figure 11: (a)Extrusion cutting slip lines field and (b) its relative hodograph. [1]

2.3 Mathematical model extrusion cutting

As for orthogonal cutting, an analysis of the process is based on the slip-line field and upper-bound theories.

However to obtain an analytical model, some assumptions must be defined. They are primarily based on the theory of plasticity where the aim is to simplify the model to a point where it can be treated easily. The assumptions that are made for the model are the followings:

- The cutting edge of the tool is considered constantly sharp.
- No deformation occurs in the material passing below the cutting edge.
- The process is operating under plane strain conditions, also known as 2D deformation.
- The friction condition on the tooling rake face is independent of the shoes positioning offset, and is expressed by the equation:

$$m = \frac{\tau}{k} \tag{2.3}$$

This means that the same friction condition is applied independent of the value of the shoe offset and can be related to m by the equation:

$$\cos(2\psi) = m \tag{2.4}$$

That friction will be assumed to be full friction, ie. m = 1.

- The workpiece is considered rigid-plastic. it means that there is no elastic. deformation or strain hardening. The material is considered perfectly plastic and it means that shear flow stress k is considered constant in the deformation zone.
- The value of the shear flow stress k is unaffected by the shoe positioning.
  Basing the following analysis on the upper-bound field shown in figure 11, it should be mentioned that the exit boundary of this field is seen to have no discontinuity line but it defines the extent of the deformation zone and of the friction contact length.
  By means of trigonometric relationships applied on the upper bound model, and using:

- The rake angle α.
- The shoe offset h (In this project it was called also feed when i'm writing about extrusion).
- The friction angle ψ.
- The tool-shoe gap S.

The first parameter to be determined is the fan angle, which is determined by the rake angle of the tool and the chip compression ratio for the specific run:

$$\tan\theta = \frac{1}{\lambda * \cos\alpha} - \tan\alpha \tag{2.5}$$

Fan angle

Based on this, the width of the deformation zone can be calculated. As the deformation zone is shaped as an elongated triangle and that the deformation takes place perpendicular to the triangle, d it is assumed to be the width of the bottom:

$$d = \frac{s}{2} * (\tan\theta - \tan\psi) \tag{2.6}$$

Width of deformation zone

After that these parameters was calculated, the shear strain during extrusion cutting can be calculated by the following equation which is based on the hodograph (Fig. 11b).

$$\gamma = \frac{u}{v_n} \tag{2.7}$$

Shear strain

This can be transmuted further by means of the hodograph

$$\gamma = \frac{\lambda}{\cos\alpha} + \frac{1}{\lambda * \cos\alpha} - 2 * \tan\alpha \tag{2.8}$$

Modified shear strain

From the equation, it can be established that the minimum possible shear strain is found when λ = 1, which is independent of the rake angle.

Based on the shear strain obtained from equation (2.8), the average shear strain rate in the deformation zone can be derived as:

$$\dot{\gamma} = \frac{\gamma * v * \sin(\alpha + \theta)}{d} \tag{2.9}$$

Shear strain rate

With v denoting the cutting speed [meters/second].

Based on these equations, the cutting power necessary to complete the process can be defined as:

$$\frac{W}{b} = kuz + mkv' * 2d \tag{2.10}$$

Necessary cutting power

Which can be transformed into

$$\frac{W}{\text{kvhb}} = \gamma + m * (\tan\theta - \tan\psi) \quad (2.11)$$

Necessary cutting power, related to fan angle

Equalling this to the dimensionless value p/k and using the prior defined equation for shear strain it gives the following equation:

$$\frac{p}{k} = \frac{W}{\text{kvhb}} = \frac{\lambda}{\cos\alpha} + \frac{1}{\lambda * \cos\alpha} - (2 + \text{m}) * \tan\alpha - \text{m} * \tan\psi \quad (2.12)$$

Extrusion pressure

Where $\cos(2\psi) = m$ as defined earlier (2.4).

The expression has a minimum value for

$$\lambda = \sqrt{1 + \text{m}} \quad (2.13)$$

Minimum value for λ

for $0 \leq \text{m} \leq 1$

Then the minimum extrusion pressure ratio becomes the following

$$\frac{\text{pmin}}{\text{k}} = \frac{2 * \sqrt{1 + \text{m}}}{\lambda * \cos\alpha} - (2+m) * \tan\alpha - m * \tan\psi \quad (2.14)$$

Minimum extrusion pressure

Gives the resultant shear stress during the cutting process for a given nominal chip compression ratio. The equivalent flow stress during the process can then be determined based on the plastic failure criterion as defined by the Tresca and Von Mises yield criterions. As the Von Mises criterion is the safer of the two in order to determined plastic deformation, the equivalent flow stress can therefore be determined by transposing σf so the resulting equation becomes:

$$\sigma_f = k\sqrt{3} \quad (2.15)$$

Flow stress from shear stress

Similarly, the equivalent strain rate and strain rate during the process can be derived by the following equations:

$$\varepsilon = \frac{\gamma}{\sqrt{3}} \tag{2.16}$$

$$\dot{\epsilon} = \frac{\dot{\gamma}}{\sqrt{3}} \tag{2.17}$$

Equivalent strain and strain rate

The temperature in the deformation zone can be approximated by the following equation, assuming an adiabatic temperature increase with the heat resulting from plastic deformation and friction work:

$$T = T0 + \Delta T \tag{2.18}$$

Temperature in deformation zone

Where ΔT can be calculated from the following equation:

$$\Delta T = \frac{k * (\frac{W}{kvhb})}{J * c * \rho} \tag{2.19}$$

Adiabatic temperature increase during extrusion cutting

With J denoting the mechanical equivalent of heat, ρ denoting the materials density and c denoting the specific heat of the material. The top part of the equation is equivalent to the extrusion pressure p determined earlier.
Based on the upper-bound analysis described here, it can be determined that extrusion cutting is a method capable of determining the shear stress of metals under the severe conditions experienced during metal cutting. This can be done with the use of the equations 2.8, 2.9, 2.12 and 2.19 which enables determination of material properties relevant for metal cutting under a wide range of strain, strain rates and temperatures. Correspondingly, the flow stress can be determined via equation 2.16 and the equivalent strain and strain rate via equation 2.17. This means that a complete data set for material properties under severe conditions can

be generated with correlation between strain, strain rates, temperature and flow stress, which can used for finite element modelling.

2.4 Current state of extrusion cutting

This thesis studies the extrusion cutting as a method to derive the flow stress of the material.

The first to theorize and to test the extrusion cutting method to obtain flow stress of material was Professor De Chiffre in 1976 [1].

He worked with brass, as its high machining index and ductility behavior made it the best candidate for the first experiments.

De Chiffre [1] worked with a 5mm thick disk, a hydraulic lathe and 2 different equipment designed by himself. In one equipment it was acquired the total extrusion force and in this way the dynamometer recorded both the force on the tool and on the shoe (Fig. 12a). The other equipment was designed to record the cutting force acting only on the tool (Fig. 12b).

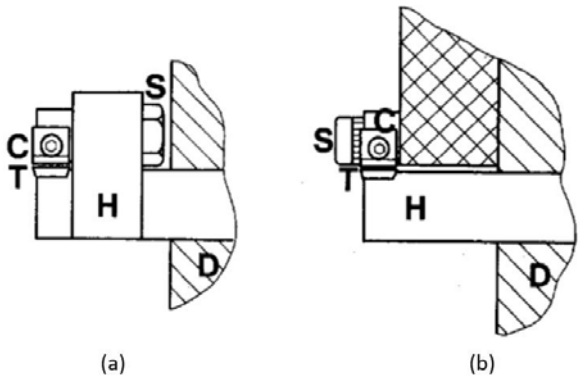

Figure 12: Set up (a) measure total tangential force, set up (b) only tool-force [1].

Where T denotes the cutting tool, C denotes the shoe, S denotes the setting screw for adjusting the gap size, H denotes the tool holder and D denotes the dynamometer. This setup proved difficult in regards to adjusting the chip compression ratio precisely.

In addition, De Chiffre [1] worked with various rake angles like 2° and 12°, with a feed of 0.25 mm, in order to obtain an experimental extrusion pressure-lambda chart that confirmed the invented theory. This would be possible If it was found a

minimum in correspondence of lambda 1.4. This happened because he discovered that curve with that point of minimum (Fig.13).

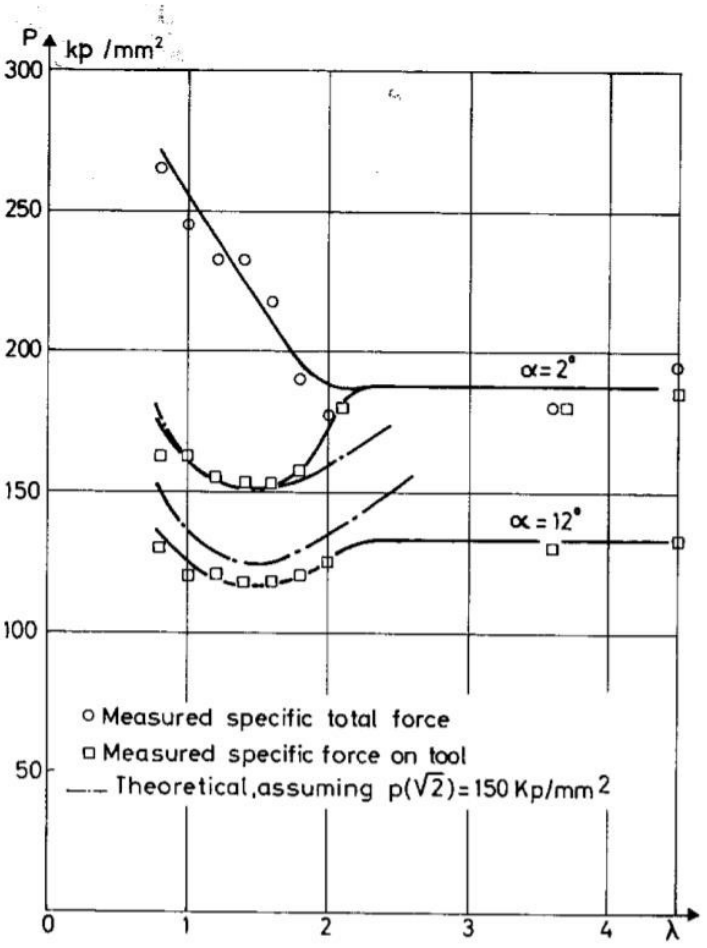

Figure 13: Ploted results De Chiffre [1]

The process was continuous and stable.

Segalina in 2016 [3], resumed the study of extrusion cutting as a method for the determination of flow stress and he tried to derive the constitutive equation of brass in turning.

Segalina[3] used brass MS63, and tried to replicate the results obtained by De Chiffre [1], using the same process parameters. However they changed the type of lathe that passed from hydraulic to electric movement, the thickness of the workpiece that passed from 5mm to 3mm, the dynamometer and the

instrumentation in general with a more modern and digital one and the equipment of the extrusion cutting that was manufactured by FATI group, which was designed only to reveal the force on the tool.
Segalina [3] obtained a curve from experimental data with a minimum point at lambda 1.4, confirming the theory (Fig.14).

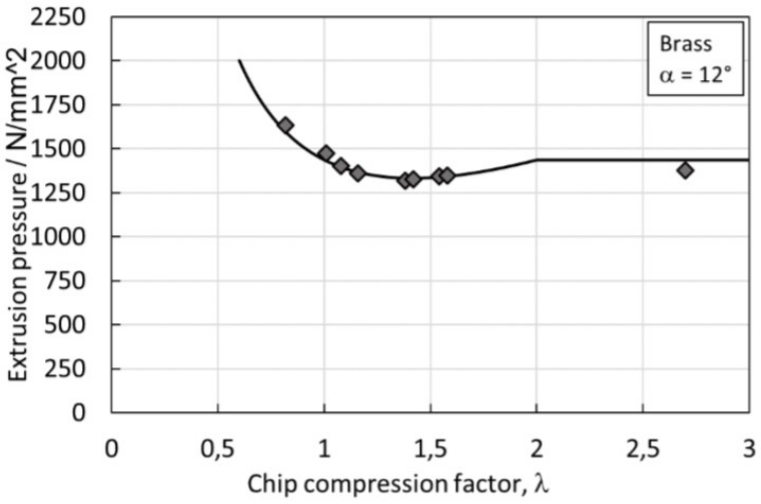

Figure 14: Extrusion pressure-lambda, Segalina 2016, [3]

With the data obtained with the brass, Segalina (Fig.14) collaborated with the computer science department. In this way they could extrapolate a constitutive equation, which was derived from a particular type of data plotting, a 4D hyper curve.
The constitutive equation obtained was inserted in a FEM turning simulation program. Segalina [3] started a simulation of an orthogonal turning process with the same conditions that he had previously performed in the laboratory.
He compared the results obtained from the simulation with the constitutive equation obtained by the method of extrusion cutting and the results of the simulation with the classical constitutive equation. Then he compared also them with the laboratory results obtained by tests. In this way it was possible to see that the simulation with the constitutive equation obtained by the extrusion cutting method gave better results and they are closer to the experimental test results.

2.4.1 Copper's test

Subsequently, Segalina and De Chiffre wrote a scientific article [5], with the aim of extending the field of extrusion cutting applicability also to another material, the copper.

They adapted the tool to the characteristics of the new material, working with a 20° rake angle.

With the copper, however, the process presented a big problem, in fact, the workpiece widened just after a few laps (Fig. 15).

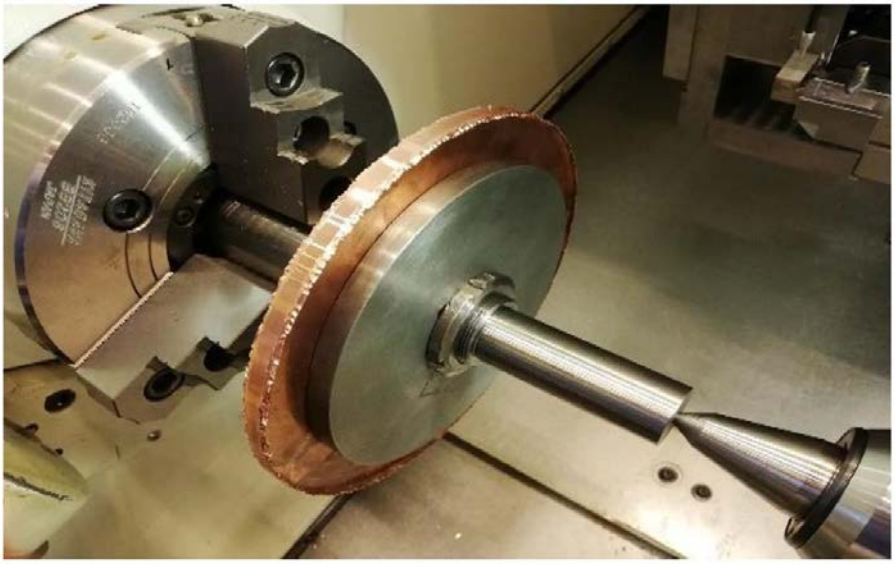

Figure 15: Workpiece in copper after a run, where is possible see the lateral widening.

This invalidated the theory of extrusion cutting, in fact, they found the minimum point at lambda 1.84.

The problem of widening (or named also lateral collapse) must be solved, in order to obtain a stable and continuous process over time.

This problem will also be the subject of the study of this thesis.

In chronological order, the work on extrusion cutting was carried out by Astrup [4] who tested the process with brass, copper and steel, but he found a lot of problems in the equipment, instruments and other also kind of problems.

That led his thesis work on the improvement of the equipment that was then manufactured by FATI, and was ready for the start of this work.

Chapter 3

3 Design of new tools and shoe

In this chapter it will be discussed the work done for the optimization design and the creation of new tools.

The parameters that have been chosen as possible causes of the errors and the non-optimal functioning of the extrusion cutting process and that was changed and improved in this work, are:

- Tool geometries
- Shoe geometries
- Cutting speed
- Feed

3.1 New copper tool

First of all, to find a solution for the widening of the copper disk, it was read a lot about the literature of turning of copper.

The problem of lateral collapse is due to too much pressure needed to extrude it, or to such an increase in temperature due to extrusion cutting without refrigerant and it would bring the metal to a softening level that would cause it to collapse. It was read scientific articles and professional turner forums on internet [6], [7], because the adjustments of the parameters of cuts such as rake angle and cutting speed could at least partially solve this problem. Perhaps the optimal solution could be the use of an abundant quantity of lubricant liquid that would have lowered the temperature of the material at the tip of the tool avoiding the effect of heat softening. In this way it would reduce the workpiece-tool-shoe friction. However this solution is impractical because the repeatability of the extrusion cutting process is still to find, and this is done by putting fewer possible variables in the process. The lubricant liquid would have been difficult to reproduce as a composition, spray direction and outlet pressure.

The studies done let understand that the frontal rake angle has a great influence on the surface finish (disk surface), and on the force necessary for cutting. Astrup [4] used a 20° rake angle for his experiments but found the problem of lateral collapse, even De Chiffre and Segalina [5] used a 20° angle.

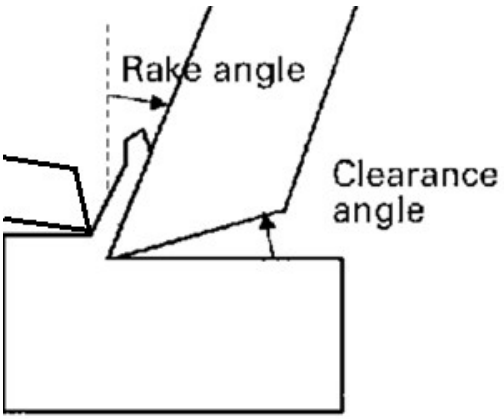

Figure 16: Image to show what is the "Rake angle" and "Clearance angle".

Assuming that with a higher rake angle see (Fig. 16), the tool penetrates better into the copper, lowering the forces and the temperatures involved. To avoid that side-collapse effect, a 25° rake angle was chosen (Fig.17) at the value limit of the recommended inclination for the turning of copper on various manuals. In their study of the optimal rake angle also take into great consideration the wear of the tool and therefore of the useful life of the tool, which is a research environment, and for this purpose is a totally irrelevant parameter.

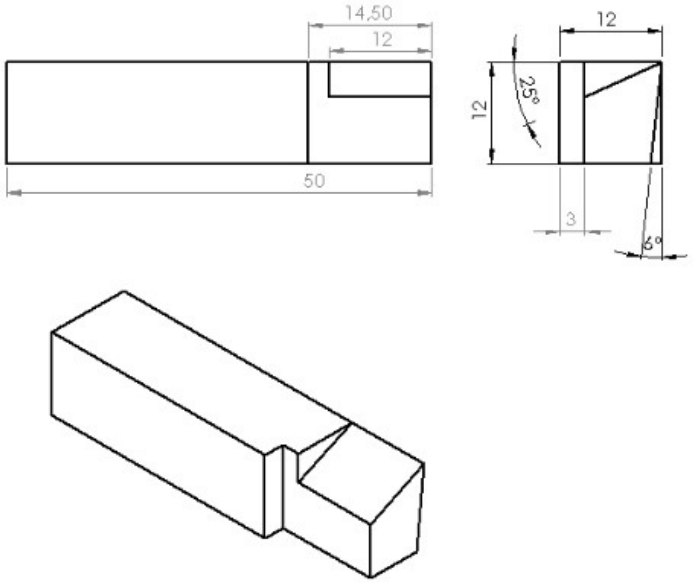

Figure 17: The copper tool with 25°rake angle.

3.2 Brass tool

The tool for the brass was chosen to use a 12° rake angle as De Chiffre [1] had previously used with excellent results and as well as Segalina in his thesis [3]. However, having done the test to insert in SolidWorks the tool for the brass in the new equipment for extrusion cutting designed by Astrup [4] and provided by FATI, was possible seen that with 12° the final part of the tool was going to close the space necessary for the evacuation of the extruded chip between tool and shoe. So the easiest and most immediate solution was to leave a 12° rake angle, but just on first 2 mm of tool are those that really work, assuming a reasonably real contact length of the chip in the 2mm, and then the rest of the tool continued with a 20° inclination (Fig. 18) so that in the terminal part closest to the shoe there was enough space for chip evacuation without problems.

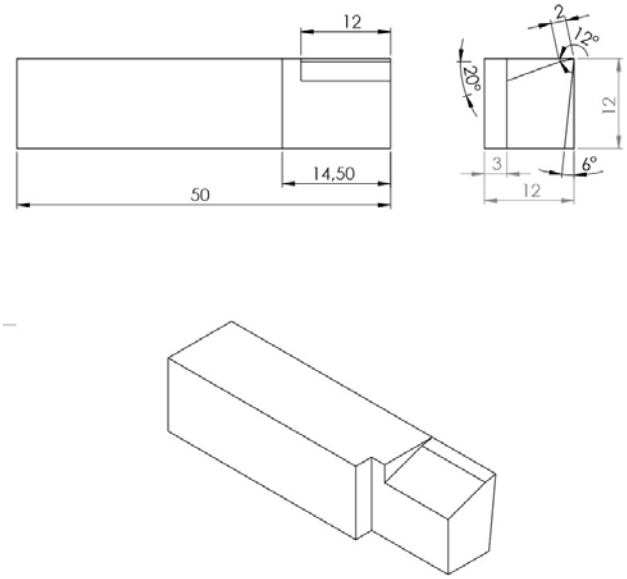

Figure 18: The brass tool with rake angle on only 2 mm and rest of the tool at 20°.

3.2.1 Clearance angle

The clearance angle was maintained at 6° as was done for all the previous tests done. The clearance angle essentially serves to avoid friction of the tool with the uncut workpiece, but if this angle is too high, the material of the tool will be reduced, with the consequence of weakening it without getting any advantages.

3.3 Shoe design

Segalina and De Chiffre in [5], tried to find the applicability of extrusion cutting on copper, as a method of characterization of the material. It emerged that the copper disk just after the beginning of the extrusion, flaked sideways (Fig. 19), increasing its width and so partially falsifying the data obtained since the area of the extruded metal was continuously increased, making difficult to identify the correct extrusion pressure.

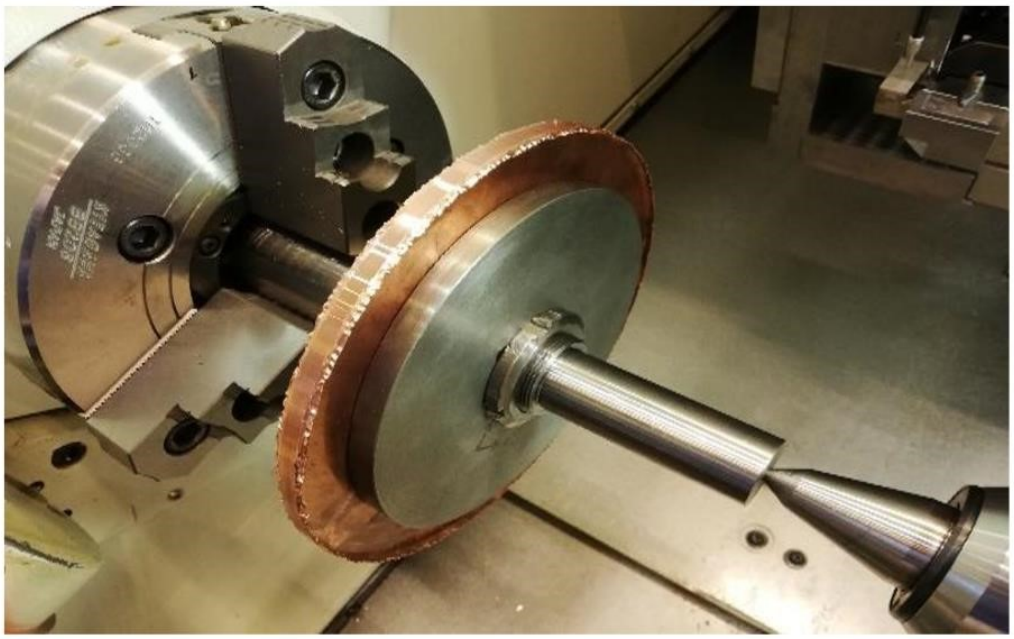

Figure 19: Wrinkled copper workpiece [4].

Astrup in his thesis [4], trying to solve this problem with the copper, inserted side shaving tools to the shoe (Fig. 20), so that these shaving tools would cut the material that had spread, keeping the copper workpiece of a constant and controlled thickness.

The idea was excellent, but the result was not so good, because the material was going to stick together with the tool and shoe and blocked the process.

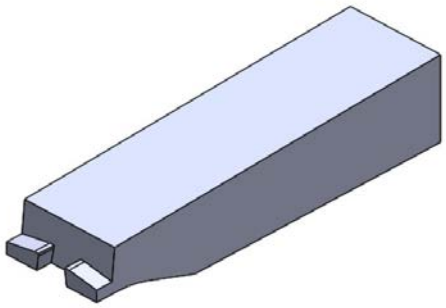

Figure 20: Copper tooling with added shaving tools [4].

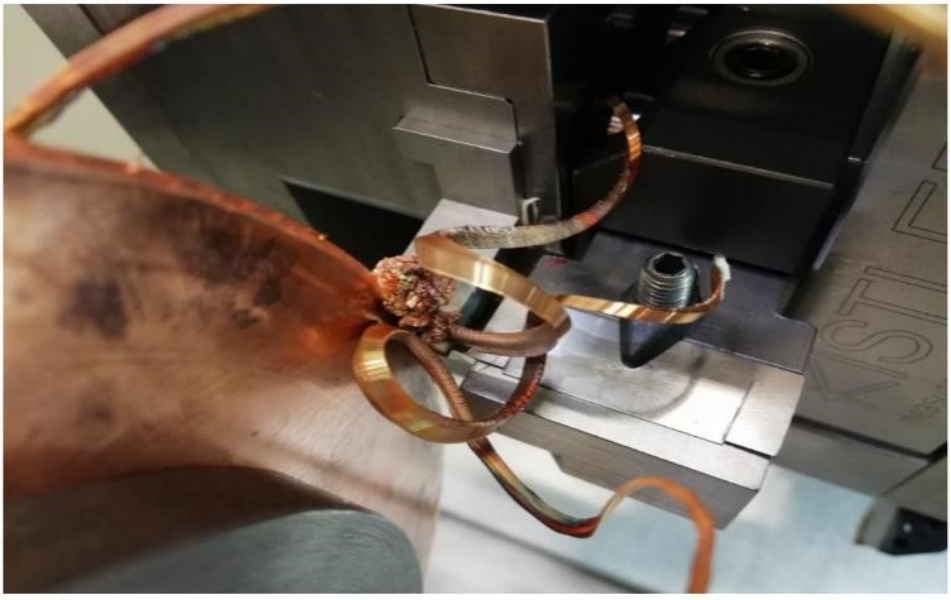

Figure 21: Destroyed copper workpiece with shaving tools [4].

With such strong evidence (Fig. 21), that the shaving tools weren't the solution, but maybe one more problem, it was eliminated, so the shoe of the copper campaign was different than the one used by Astrup [4]. In the tests that were done, was used the same shoe also used for brass.

A cause of process failure was the material pile-up on the shoe. Astrup [4] passed from the 2 degrees of entrance angle of the shoe used by De Chiffe and Segalina [1],[3],[5], to 5°, thinking that there was less workpiece-tool contact, but with his experiments a bad effect was noticed. The material that accumulated on the shoe was so much that it increased the force on the shoe until pushing it down and closing the gap shoe-tool and blocking the process. This failure mode can also be attributed to an incorrect design of the equipment, which Astrup [4] later modified designing a new version of shoe-holders.

To still avoid the accumulation of material, was opted for an entrance angle of the shoe of 2°, exactly like that used by Segalina and De Chiffre [5] with "excellent" results.

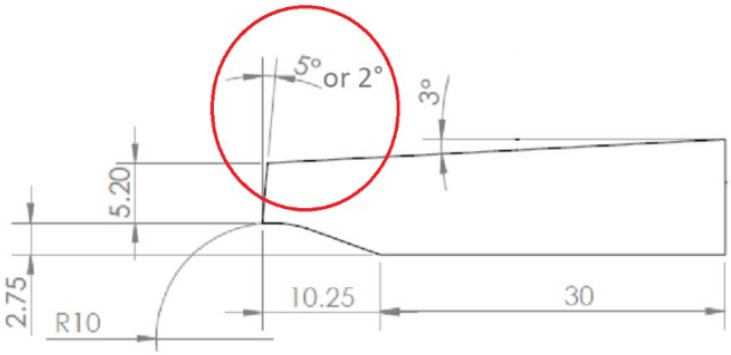

Figure 22: Shoe showing entrance angle of 2°, or 5° [4].

3.4 Tools material

The "old" tools were produced from ASP 60 high-speed steel bars, and the shoe also with the same material, while for the new experiments it was decided to use an HSS 30 which in comparison to the ASP 60 is more tenacious even if it has a lower wear resistance. However for the purpose of this work and the materials used to work, copper and brass, it is better and the tool life is the last of the parameters to be taken into consideration and the priority is to obtain a stable process.

Tugsten carbide was also available but it will be used for the test on steel, as it makes no sense to use the material so hard and difficult to sharpen as carbide for relatively soft materials such as copper and brass.

Chapter 4

4 Extrusion cutting instruments and equipment

In this chapter all the instruments used during the laboratory tests will be described in detail, including the equipment (Fig. 23).

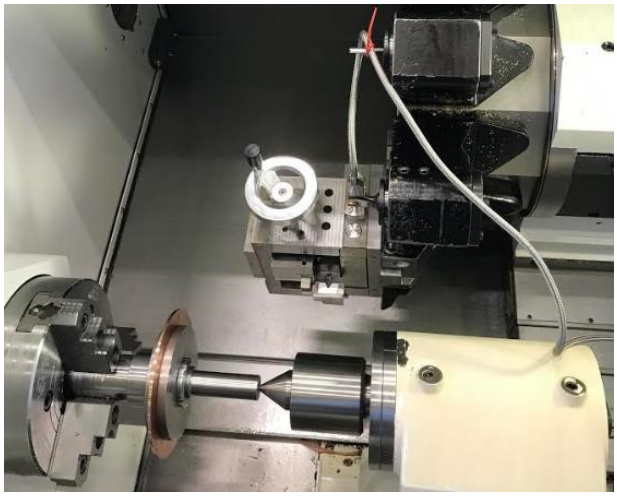

Figure 23: Extrusion cutting equipment.

4.1 Dynamometer

Kistler 9129AA Multicomponent dynamometer was used (Fig. 24) It is capable of measuring forces in three different directions, namely the X, Y and Z-axis (Fig. 25). Respectively cutting force, trust force and z force.

The force sensors each contain three crystal quartz disks, one of which is sensitive to pressure in the y direction and the two others to shear force in the x or z directions. The forces are measured with practically no displacement.

The directions of these forces are specified relative to the front of the dynamometer, as illustrated in the figure 24.

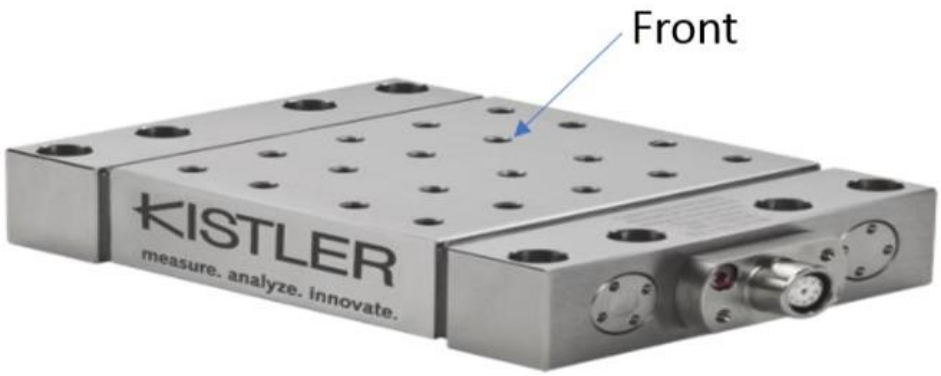

Figure 24: Illustration of dynamometer including front area.

and the positive measurement directions are illustrated in the figure 25.

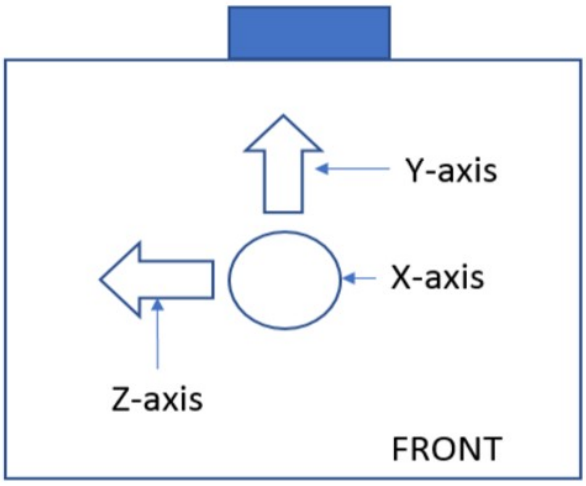

Figure 25: Illustration of force measurement directions relative to the front of the dynamometer, as illustrated in figure 24.

Max. permitted measuring range

	Fx, Fy, Fz	–10 ... 10 [kN]

(Force application point at cover plate surface)

	Mx, My, Mz	–500 ... 500 [N·m]

Sensitivity (rated)

Fx	pc/N ≈–8,1
Fy	pc/N ≈–4,1
Fz	pc/N ≈–8,1

Natural frequency

fn(x)	kHz ≈3,5
fn(y)	kHz ≈4,5
fn(z)	kHz ≈3,5

With copper and brass extrusion, from [3], [5] is possible to notice that the forces involved are not greater than 2000N and therefore there is no problem of damage the dynamometer having a limit for 10000N. A different case is if the steel is extruded; the forces would be much higher and to preserve the dynamometer's integrity the design of a notch designed on the tool would be necessary so that at a certain level of force reached the tool would break and not the dynamometer which is more expensive.

The natural frequency of the system and dynamometer are to be observed because if it was reached the same frequency, the signal of the forces would result infinite, reaching the resonance.

The dynamometer is mounted on the main structure of the dynamometer using four M5 machine screws. On the flat surface of the dynamometer there are multiple blind bores available, for which a tooling slot is mounted, which in turn mounts the tool bit holder. For the calibration certificate of the dynamometer, see appendix.

Charge amplifier channels are also needed to build a complete measuring.

4.2 Charge amplifier

Figure 26: Multichannel laboratory charge amplifier Type 5070A.

This universal laboratory charge amplifier (Fig.26) can be used for force and torque measurements with piezoelectric dynamometers or force plates. Piezoelectric sensors produce an electric charge which varies in direct proportion with the load acting on a sensor. The amplifier converts this charge signal into a proportional output voltage.

This instrument is particularly suitable for general force measurements, cutting force measurements with Kistler dynamometers when a wide measuring range or high quality of signals is needed.

Figure 27: Data Acquisition System for Force Measurement Type 5697A.

The DAQ system for DynoWare (Fig. 27) consists of a connection box and the DynoWare program. Up to two multichannel charge amplifiers, and hence two measuring chains, can be connected to the connection box A 16-bit A/D converter digitizes the analog output data. The system is connected to the PC via a USB 2.0 port, control of the charge amplifier or signal conditioner is handled by the connection box via an RS-232C cable.

Users have at their disposal an easy-to-use data acquisition system with a high sampling rate.

5697A DAQ system has been developed specifically for piezoelectric measuring systems and their charge amplifiers and signal conditioners. The excellent resolution of the system and its very high sampling frequency of up to 125 kS/s with 8 measuring channels enables customers to measure highlydynamic processes and covers a very broad range of applications. When it is used in conjunction with the DynoWare package, the DAQ system comes into its own in general measuring and cutting force measurement applications.

					
Dynamometer	Connection cable, high impedance	Charge amplifier	Connecting cable	DAQ system	Notebook (from customer side) with DynoWare
Type 9129AA	Type 16xx	Type 5070A	Type 1700A111A2 Type 1200A27	Type 5697A1	

Figure 28: Typical measuring chain with DAQ system Type 5697A1.

4.3 Software

Figure 29: Laboratory Virtual Instrument Engineering Workbench (LabVIEW).

It is a system-design platform and development environment for a visual programming language from National Instruments.

4.3.1 Software setting

The most important part of measuring chain to get good data is the LabVIEW setting.
So in this part it will be explained how it was set up and how is used the step data acquisition program.

The dynamometer cables have thus been connected
Channel # 1 - A0 which corresponds to the X axis
Channel # 3 - A1 which corresponds to the y axis
Channel # 5 - A2 which corresponds to the z axis

Turn on the Channel Change Amplifer Type 5070
Selecting channel # 1 makes it possible to see that it is set to 5000N by default, so the gains, that indicates the scale factor is 500N/V. This means that if the dynamometer perceives 500N, the amplifier will send 1 volt signal having a scale factor of 500N/V.
Knowing that the forces in the channel involved would reach a maximum of 1000N, setting 1000N in that specific channel, one would get a gain of 100N/V

and thereby have to manually set the value of "100" in the box for that channel's gain in that channel in LabVIEW program.

- Open LabVIEW 2016 (Fig. 29)

It is now possible to see that on the left there are some panels called "Gain" and there are as many boxes as there are connected channels, in these experiments, case 3.
So having set the amplifier to the value of 5000N on channel #1 (axis X) corresponding to a gain of 500N/V, one must also set this value of Gain in LabVIEW in correspondence of Gain X.

A problem arises when the maximum force is set to 1000N but eventually reaches a greater force. This will contribute to the appearance of an horizontal line, as it went off the scale. It is important to be aware of the fact that the dynamometer has an upper limit of 10 000 N. Exceeding this limit it would be possible the breaking of the dynamometer.

With "cctrl + E" the block diagram opens where there are all the important functions.
The block on the left is the one that reads the data.

From this block, it is possible to see the channels that acquire that are A0, A1, and A2., then you see the range that was pre-set at ±10 V and that is fine for the experiment. Then there is the way of acquiring data, acquisition mode.
"Continuous sampling" is chosen, which means that it acquires data continuously from when it starts shuffle and until it stops.
And then there is the acquisition speed which was set at 20000Hertz (on the advice of a Ph.D. was kept this value, but then it turned out to be catastrophic because it weighed down my data analysis making the Excel stops working)

4.4 Caliper

Figure 30: Diesella digital caliper 0-150 mm x 0,01 mm

Measuring range	0-150 mm
Resolution	0,01 mm
Accuracy	± 0,03 mm
Jaw length	40 mm
Material	Stainless steel

Table 2: Caliper characteristic

4.5 Work piece

Figure 31: Brass workpieces in different size.

Circular workpieces (Fig. 31) with thickness equal to 3mm were realised cutting a MS63 brass sheet and pure copper half hard sheet (2000x1000x3mm) with water-jet and then turning them to a diameter of 210mm. One mounting hole, Ø37, was cut in the middle of the disc to enable fitting the workpiece to the mandrel already existing, and other two holes, Ø6, were also cut to the sides of the mounting hole to enable the fitting of pins into the workpiece, so that support rings could be mounted, to reduce the amount of vibrations occurring and give stiffness on workpiece. Mainly used discs already used for a few runs by Segalina [3] and Astrup [4], I made a sort of recycle of old workpieces that were still excellent with a diameter between 205mm and 180mm they still had many runs to do. Obviously, before starting this tests it has been preventively turned with a "normal" orthogonal cutting to reach the roundness.

4.5.1 Properties of metals used

Properties MS63 brass Cu69/Zn37	
Electrical Properties	**Value**
Electrical resistivity (µOhmcm)	6.2-6.6
Temperature coefficient (K^{-1})	0.0016-0.0017
Mechanical Properties	
Elongation at break (%)	<55
Hardness - Brinell	65-136
Modulus of elasticity (GPa)	95-110
Shear strength (MPa)	280-310
Tensile strength (MPa)	330-500
Physical Properties	
Density (g cm^{-3})	8.45
Melting point (C)	900-920
Thermal Properties	
Coefficient of thermal expansion @20-100C ($x10^{-6}$ K^{-1})	19.0-20.5
Thermal conductivity @23C (W m^{-1} K^{-1})	125

Tables 3: Brass properties

Properties pure copper half hard	
Physical Property	**Value**
Density	8.92 g/cm³
Melting Point	1083 °C
Thermal Expansion	16.9 x10^-6 /K
Modulus of Elasticity	117 GPa
Thermal Conductivity	391.2 W/m.K
Electrical Resistivity	0.0203 x10^-6 Ω .m
Sheet - 3mm thick	
Mechanical Property	**Value**
Proof Stress	50-340 MPa
Tensile Strength	200-360 MPa
Elongation A50 mm	50-5 %
Hardness Vickers	40 to 110 HV

Table 4: Copper properties

4.6 Support disks

Support disks in steel (Fig. 32), with variable diameters and 10mm thick, were designed to prevent workpiece deflection during the process.

The workpieces are only 3mm thick, with a high ratio value of diameter on thickness and have a modulus of elasticity that is not very high for both materials, copper and brass. The workpiece tends to vibrate and to flex during the process, so these disks have been made of support in order to stiffen the workpiece closing in a sandwich.

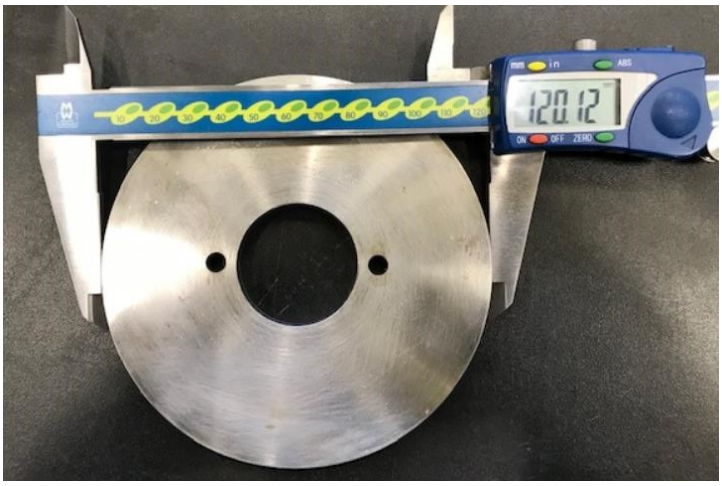

Figure 32: Support disks in steel used for extrusion cutting

The support disks are made with decreasing diameters to follow the reduction of the diameter workpiece. The difference between the workpiece and the support disks reaches 20mm on the diameter. The spindle is disassembled and the support disks are changed with two smaller ones and then reassembled on the lathe for new runs. This is to avoid the collision extrusion cutting equipment-support disk.

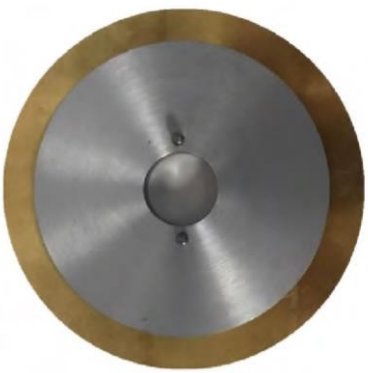

Figure 33: Assembly workpiece-support disks. [3]

4.7 Lathe

The operations of cutting were carried out on the Mazak Nexus CNC lathe

Figure 34: The Mazak Nexus CNC lathe

4.8 Mandrel

The mandrel had prolongation of 72 mm in order to prevent the contact with the lathe revolving head and the tail stock, necessary for increasing the system stiffness and reduce workpiece vibrations so improve process stability with a vibration-free force diagram. Additionally, two holes were realised for pins' insertion, necessary to fix workpieces.

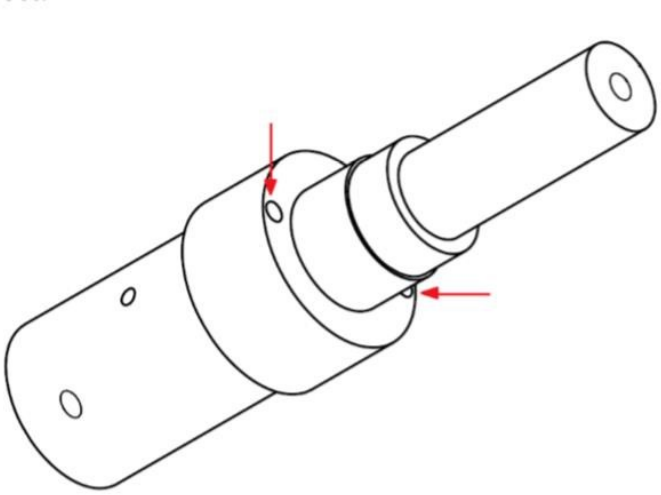

Figure 35: Extrusion cutting mandrel with focus on two holes for pin's insertion [3]

4.9 Main Equipment

The equipment used by Segalina [3] was "raw" and at the early stages of development, then Astrup [4] in his thesis found some problems with the equipment, and then set his thesis work on design improved equipment. In these tests was possible to take advantage of the new equipment that worked very well, it was able to achieve the hoped-for process stability.

To know in detail all the parts of the equipment, see the thesis of Astrup [4] and Segalina [3].

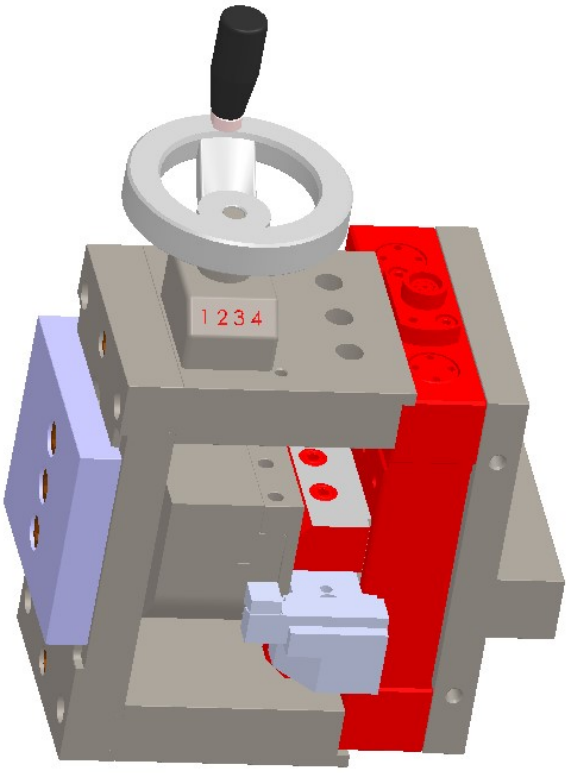

Figure 36: New equipment provided by Fati group, updated to 2019 after the new re-design made by Astrup [4]

Chapter 5

5 First experimental test campaign

In this chapter it will be discussed about the laboratory tests that was made, first on brass and then on copper.

It was started with a brass test because it is the material on which more tests have been made, and it is the one where the process is more stable.
It was kept the parameters already positively tested by Segalina [3] and Professor De Chiffre [1]. They are the follows:

- same feed, equal to 0.25mm.
- same material, brass.
- same cutting speed.

The purpose of the first experimental campaign is to test the changes made on the equipment by Astrup [4] and manufactured by FATI group. Which should have led to an easier and more effective adjustment of the gap between shoe and tool.
The operator started by assembling the equipment first on the work table and then positioned on the lathe.
Then very carefully the dynamometer was connected and it was also bound the dynamometer cable outside the lathe to avoid that falls or is unintentionally break, being a new and very expensive cable. It was subsequently checked that the high between the tips was right to avoid trivial errors.

Phases of the procedure in general:

• Work piece placed between support disk and clamped on the mandrel;
• Charge amplifier turned on from reset to measuring mode;
• LabVIEW software started on a PC (forces data acquisition);
• Extrusion cutting operation;
• LabVIEW program stopped, charge amplifiers turned to reset mode;
• Tool inspected (wear and build up edge detection);
• Shoe cleaning with abrasive paper (removal of residual brass);
• Chip collected in numbered envelopes;
• Forces, Chips thickness evaluated.

5.1 Set up of the first experiments on brass

At the beginning of the test, on the first day, the purpose was to verify the new equipment and to increase the efficiency of the test. So it was exploited every run also for the acquisition of new data useful to get robust the extrusion cutting process.
It was seen that the operator needed from 5 to 10 minutes to change the set up of the gap between the shoe and the tool. On the other hand, it was seen that to change the CNC's program on the machine was faster. In order of tens of seconds, it was set before every run the rotation speed based on the last diameter, using the formula:

$$n = 1000 * \frac{V}{\pi} * \frac{1}{D} \qquad (5.1)$$

It was clear that the "bottleneck", which is the part that slow down the process, in the speed of testing was used to adjust the shoe-tool gap. It was decided that this parameter had to be changed as little as possible.
It was decided to do two experimental campaigns in one step, that is with a cutting speed of 80m/min and another with 100m/min. In this way, changing the shoe-tool gap only once it could be possible to get twice as much data with just one shoe setting.

It was possible to get the data of 30 different lambda-cutting speed combinations in a single test day.

5.2 Set up of the first experiments on copper

On the second day it was done the most difficult test, that is on copper. Astrup's tests [4] on this material were not so good because the material continued to stick to the tool (build up) or the chip was embedded between the shoe and the tool. The consequence was the problem of the lateral collapse, also found by Segalina and professor De Chiffre [5] when they extruded copper.

Nevertheless, it was prepared several worksheets to base the experiment. It was chosen three different cutting speeds and three different feeds for each speed, because it was thought that the most problems were due to non-optimal process parameters.

It was investigated the cutting speed of 80m/min because with the brass it had given excellent results, then 100m/min because in [5] was used this speed. It was also tried to push the experiment up to 120m/min even if it is a speed not recommended for an HSS tool because it is too high and drastically reduces tool life, but on the other hand it has the advantage of reducing the forces.

For the feed, it was used 0.25 mm because for the brass it gave excellent results and with 0.20mm because Segalina [3] worked with this feed. It was used also 0.18mm to try to reduce the forces involved avoiding the lateral collapse. This is because working with smaller feeds reduce the cutting force.

But at the same time if the feed is reduced too much the influence of the micrometric roundness of the tool tip starts to be influential going to change the rake angle.

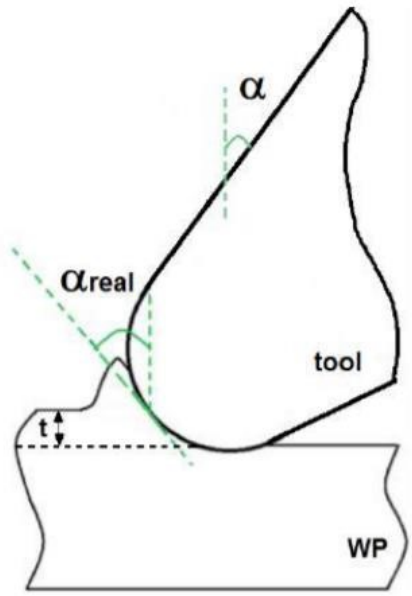

Figure 37: Schematic representation of the tool tip with small feed.

In figure 37, it is easy to understand that if the feed is very small, it will modify a fundamental parameter for the calculations, and so the rake angle, which from positive can even become negative as shown (Fig.37).
For each of these combinations it should be used at least 10 gaps to have enough data that can be used for data processing.

5.2.1 Strategy to choose best parameters for copper

To have at least 10 different gaps was not compatible with the time available to the machine and the operator, so the strategy (Tab.5) was to do runs initials with a 1.8 lambda that would be the lambda value that Segalina and De Chiffre [5] found. It was of minimal extrusion force (although the theory says it should be wrong, should be at a lambda 1.4). Using this lambda, it was made 9 different tests, with 3 different feeds and then it was changed the gap for each feed. Moreover for each of these, it was used a run for each cutting speed 80, 100 and 120 meters per minute. Before each start, it was measured the thickness of the disk, and again at run finished with the aim of identifying the combination of best cutting parameters that was chip quality, lower lateral collapse and "work noise"

Feed 0,25mm				Wide	
test	λ	GAP	speed m/min	start	finish
1	4,8	1,2	80		
2	2,5	0,625	80		
3	2,5	0,625	100		
4	2,5	0,625	120		
5	2,2	0,55	80		
6	2,2	0,55	100		
7	2,2	0,55	120		
8	2,0	0,5	80		
9	2,0	0,5	100		
10	2,0	0,5	120		
11	1,8	0,45	80	4,95	5,6
12	1,8	0,45	100	4,9	4,95
13	1,8	0,45	120	3,55	4,9
14	1,6	0,4	80		
15	1,6	0,4	100		
16	1,6	0,4	120		
17	1,4	0,35	80		
18	1,4	0,35	100		
19	1,4	0,35	120		
20	1,2	0,3	80		
21	1,2	0,3	100		
22	1,2	0,3	120		
23	1,0	0,25	80		
24	1,0	0,25	100		
25	1,0	0,25	120		
11,2	1,8	0,45	60	3,9	4,8

Feed 0,2mm				Wide	
test	λ	GAP	speed m/min	start	finish
1	4,8	0,96	80		
2	2,5	0,5	80		
3	2,5	0,5	100		
4	2,5	0,5	120		
5	2,2	0,44	80		
6	2,2	0,44	100		
7	2,2	0,44	120		
8	2,0	0,4	80		
9	2,0	0,4	100		
10	2,0	0,4	120		
11	1,8	0,36	80	4,8	6,02
12	1,8	0,36	100	6	6,92
13	1,8	0,36	120	4,2	5,6
14	1,6	0,32	80		
15	1,6	0,32	100		
16	1,6	0,32	120		
17	1,4	0,28	80		
18	1,4	0,28	100		
19	1,4	0,28	120		
20	1,2	0,24	80		
21	1,2	0,24	100		
22	1,2	0,24	120		
23	1,0	0,2	80		
24	1,0	0,2	100		
25	1,0	0,2	120		

Feed 0,18mm				Wide	
test	λ	GAP	speed m/min	start	finish
1	4,8	0,864	80		
2	2,5	0,45	80		
3	2,5	0,45	100		
4	2,5	0,45	120		
5	2,2	0,396	80		
6	2,2	0,396	100		
7	2,2	0,396	120		
8	2,0	0,36	80		
9	2,0	0,36	100		
10	2,0	0,36	120		
11	1,8	0,324	80		
12	1,8	0,324	100	3,4	4,8
13	1,8	0,324	120	3,3	5,3
14	1,6	0,288	80		
15	1,6	0,288	100		
16	1,6	0,288	120		
17	1,4	0,252	80		
18	1,4	0,252	100		
19	1,4	0,252	120		
20	1,2	0,216	80		
21	1,2	0,216	100		
22	1,2	0,216	120		
23	1,0	0,18	80		
24	1,0	0,18	100		
25	1,0	0,18	120		

Table 5: Second experimental copper campaign was set up

After a visual analysis, it was chosen the feed 0.25mm and cutting speed 100 and 120m/min.

The 0.2 mm and 0.18 mm feeds widened a lot, while the 80m/min speed was the one that gave the less good chips, to confirm that low cutting speeds had a negative effect in the extrusion cutting process was made also a run at 60m/min. This confirmed that the high speeds were a good choice. As for the lateral widening, a scientific method was not followed because it was always started from a different disk width. The reason why is that the operator should have disassembled the spindle with the disk and mounted it on manual lathe in order to remove the excess copper in the sides. It could not take advantage of the CNC turret where it is performed the experiments because it could not rotate because the dynamometric cable passed precisely around the turret. So the lateral cleaning of the disc took up a lot of time and therefore this operation was done only at every feed change.

5.2.2 CNC's program to have the costant disk thickness in the beginning

So before starting the real experimental campaign with 0.25mm feeds and the two speeds at 100m/min and 120m/min, it was created a program by Landerghini for the CNC. It allows to clean the surface of the disk from the material on the sides without disassembling the disk and do this on the manual lathe.

This program consists of a 2mm turning/removing on the diameter with a feed of 0.05mm so with any gap tool-shoe is set. It is possible only to have a normal orthogonal turning without extrusion, and in addition, a so low feed is suggested by manuals as the best surface finish parameter.

While for the cutting speed it was chosen 100m/min, this speed for surface finishing is also recommended as the most suitable for having an excellent surface finish. Therefore, after the completion of the extrusion cutting operation, the data acquisition by the dynamometer was stopped, and it was possible to open the Mazuck's safety window, to extract the extruded chip with pliers, being careful to the very high temperature of it. Finally, it was possible to close the safety window and start the second part of the program that provides for the elimination of the lateral material. Thus, at each start, there was a disk of almost constant thickness for each run.

This was how we proceeded, feed set to 0.25mm and two runs for each of the cutting speeds for each lambda.

With copper, after the experience of brass, it was preferred to choose lambda a little more sparse than with brass. The reason why was there was an uncertainty in the hundredths millimetre of the gap. It was difficult for the operator to find all the necessary thickness gauges. In any case, the extruded chip measurement had always an uncertainty of a few hundredths of millimetres of thickness. Therefore, it was useless to try to get and then to plot uncertain points.

5.3 Chip collection and cataloguing

Each chip was taken by the operator with pliers because of the high temperature reached; they were placed on a wooden work table for a few minutes to cool down until it was possible to handle them manually. Each chip was inserted in a plastic bag, on which the test number was previously written in order to identify them. It was also written the nominal lambda, the gap, the initial diameter of the disc, the final diameter. Moreover, it was also indicated if the chip during the extrusion made a strange noise, because in the case that in the post-processing the graph of the forces had been not uniform, it could have been due to this noise or any other parameters.

5.4 Tool wear and build-up effect

A visual examination of the cutting edge of the tool at the end of the experiment day (Fig.38) reveals that the tool has no visible sign of wear, and no accumulation of material, neither on the tool nor on the shoe.

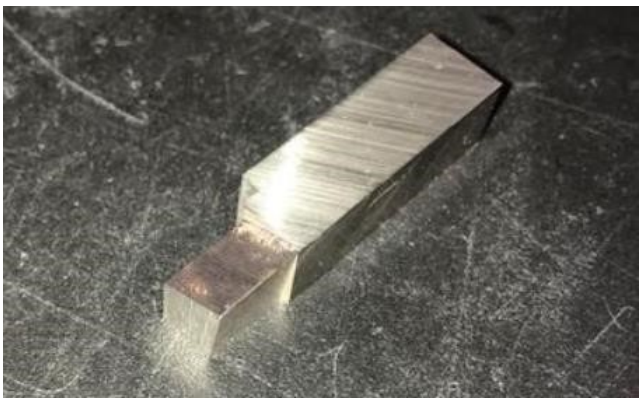

Figure 38: Cleaned tool after a lot of runs of extrusion cutting

A more accurate analysis was undertaken, inspecting the cutting edge with the help of an optical microscope.

This strategy didn't give any good results because the HSS tools are very shiny, and a microscope that uses light to define the image has problems, mostly to analyse the rake angle that is obviously inclined, since it is formed by the intersection of the rake angle and by the clearance angle.

5.5 Chips dimension analysis

The chips are 1m to 2m long, depending on the size of the disk reached when they were extruded and the lambda used for that test.

$$lenght_{chip} = \mathrm{D} \cdot \pi \cdot \frac{D-d}{h \cdot \lambda} \tag{5.2}$$

Where:

D = initial diameter

d = final diameter

h = feed

λ = chip compresion

Before the measurement, the calliper was tested for bias with a gauge block of 1 mm thickness, where no bias was determined. The measurements were taken in a room with temperatures ranging from 22 to 24 Celsius degrees during the measuring session.

Each chip has minimal variations in thickness and width in its length (Fig. 39),

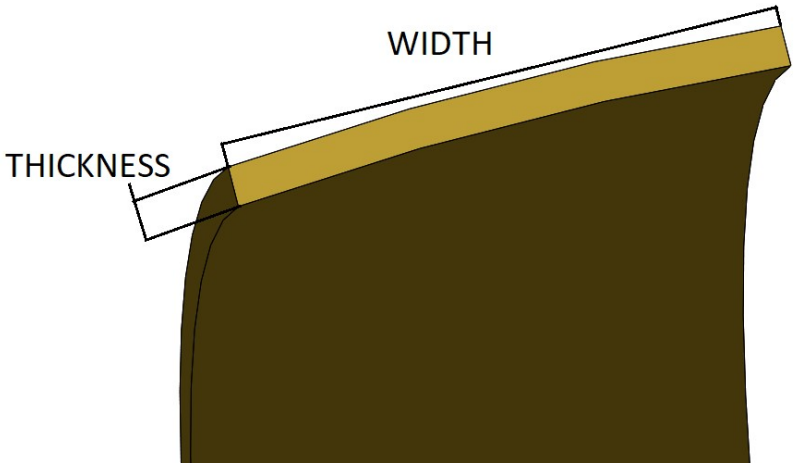

Figure 39: This figure show what is meant for thickness and width.

with the measurement of chip thickness, it is possible to see if the process is stable or if there are any variations due to the opening or closing of the gap tool-shoe during the process.
Moreover, it is of fundamental importance the width measurement.
The aim of experiment is to see if the extrusion pressure-chip compression curve has or not a minimum in corresponding lambda 1.4 for the brass. For this reason, it is very important to obtain the real and average extruder pressure of the chip.
To obtain the extrusion pressure of the chip it was used the cutting force obtained by plotting the dynamometer data, divided by the area of the chip, which, being rectangular, is obtained by multiplying width by thickness. The thickness is constant, fixed at 0.25mm because it is the feed, while the width varies slightly because the disk tends to widen even with the brass although only a few hundredths of a millimetre, but in any case, this influences the calculation of the pressure.

5.5.1 Chip area

To derive the area, it was taken the chips and it was identified where the actual extrusion process began and where it ended. This is the introduction and exit area of the tool on the disk, and it was divided into three parts, beginning, centre, and end, for each of these 3 points thickness and width have been obtained.
But there was the problem that the chip was curved (Fig. 40) and if it was not measured a completely flat area, the measurement could be wrong, even more, the width because with the calibre it was to take the sides in a perfectly perpendicular way to have the right measures (Fig. 41).

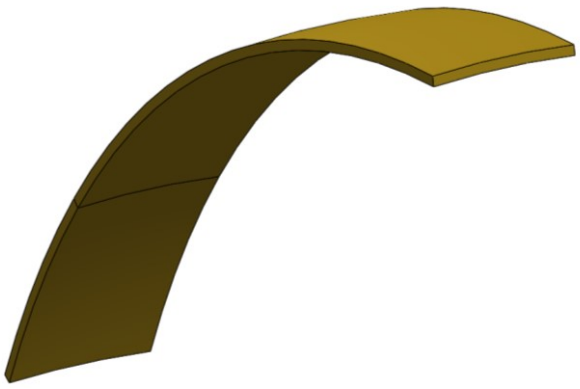

Figure 40: Tipical chip shape.

In each point, 5/6 measurements were taken at a distance of a few millimetres in order to see which was the most correct measure, and if this measure was the one reported for data analysis.

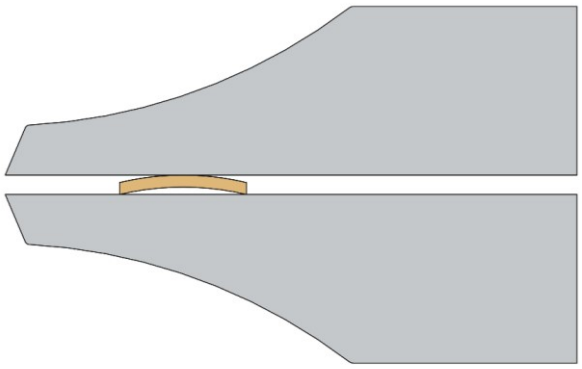

Figure 41: Where a random uncertainty of the measure comes from, calliper and chip.

5.6 Force analysis

The data acquisition program, LAB VIEW, was set to work with a data acquisition frequency of 20kHz, on 3 channels, one for the cutting force, one for the z force and one for the thrust force.

The data is in lvm format and it has been analyzed with the Microsoft Excel program. Once opened it was immediately noticed that they were all negative, so it was necessary to transform these data into an absolute value. This operation is certainly not easy, because it is about a million lines by 4 columns, the fourth column is time, a quantity of such data is heavy enough to be processed with excel and the problem cannot crash the program. The solution is to plot only the time and cutting force column, which is what is needed to get the pressure. Therefore it was seen which part of the data is interested for our test and all the lines that are not needed were removed. In this way, the remaining data have been taken in absolute value and plotted. The cutting force part was also divided into 3 parts, beginning in the middle and ending, and the force was read in these three points to be able to divide it by the area corresponding to those 3 points. This was done for

all the chips and two different Excel worksheets were created, one for the cutting speed of 80 m/min and one for the cutting speed of 100m/ min. Then 3 pressures per chip were calculated and the average of these 3 pressures was made.

imposed Λ	indicates the imposed lambda ie gap shoe-tool / feed
t [mm]	is the thickness of the chip
w [mm]	is the width of the chip
Area [mm^2]	is the area of the chip's extruded section obtained by multiplying t x w
Fc [N]	is the cutting force read by the dynamometer
P [MPa]	is the extrusion pressure obtained by dividing the cutting force by area obtained by multiplying feeds by width
Ave P [MPa]	is the average extrusion pressure on that chip
Ave t [mm]	is the average thickness in that chip
actual λ	is the true lambda obtained by knowing the average chip thickness that corresponds to the true gap

Table 6: Legend chart

Test cutting speed 80m/min

Imposed λ	t [mm]	w [mm]	area [mm^2]	Fc [N]	P [MPa]	Ave P [MPa]	Ave t [mm]	actual λ
	0,51	3,74	0,9	968	1035			
2,2	0,54	3,87	1,0	936	967	990	0,50	2,00
	0,45	3,8	1,0	920	968			
	0,5	3,5	0,9	845	966			
2	0,47	3,85	1,0	810	842	879	0,47	1,87
	0,43	4,1	1,0	850	829			
	0,46	3,9	1,0	927	951			
1,8	0,4	3,91	1,0	980	1003	978	0,44	1,76
	0,46	3,7	0,9	908	982			
	0,42	3,85	1,0	855	888			
1,7	0,42	3,95	1,0	865	876	882	0,42	1,68
	0,42	3,95	1,0	870	881			
	0,39	3,95	1,0	874	885			
1,6	0,38	4	1,0	885	885	879	0,37	1,47
	0,33	4,2	1,1	909	866			
	0,34	3,93	1,0	931	948			
1,5	0,32	4,05	1,0	927	916	928	0,32	1,28
	0,3	4,2	1,1	967	921			
	0,31	4,41	1,1	1100	998			
1,4	0,28	4,45	1,1	1150	1034	1010	0,29	1,16
	0,28	4,8	1,2	1200	1000			
	0,3	3,98	1,0	1029	1034			
1,3	0,26	4,5	1,1	1162	1033	1029	0,29	1,17
	0,32	4,28	1,1	1090	1019			
	0,3	4,36	1,1	1020	936			
1,2	0,26	4,7	1,2	1215	1034	969	0,27	1,08
	0,25	4,4	1,1	1030	936			
	0,28	4,05	1,0	1020	1007			
1,1	0,27	4,11	1,0	1086	1057	1015	0,27	1,09
	0,27	4,2	1,1	1030	981			
	0,25	4,17	1,0	1020	978			
1	0,25	4,31	1,1	1150	1067	1009	0,27	1,07
	0,3	4	1,0	980	980			
	0,26	4,28	1,1	1000	935			
0,9	0,22	4,48	1,1	1170	1045	972	0,24	0,97
	0,25	4,27	1,1	1000	937			
	0,24	4,36	1,1	1000	917			
0,8	0,2	5,1	1,3	1400	1098	968	0,21	0,85
	0,2	4,5	1,1	1000	889			
	0,18	4,7	1,2	1180	1004			
0,7	0,25	5,2	1,3	1500	1154	1060	0,22	0,87
	0,22	4,7	1,2	1200	1021			

Table 7: Results first experimental campaign brass, cutting speed 80m/min.

Test cutting speed 100m/min

Imposed Λ	t [mm]	w [mm]	area [mm^2]	Fc [N]	P [MPa]	Ave P [MPa]	Ave t [mm]	actual λ
	0,49	3,86	0,97	1100	1140			
2,2	0,48	4,22	1,06	950	900	997	0,48	1,93
	0,48	4	1,00	950	950			
	0,5	3,7	0,93	820	886			
2	0,5	3,7	0,93	925	1000	937	0,50	2,00
	0,5	3,75	0,94	867	925			
	0,43	3,81	0,95	860	903			
1,8	0,45	3,84	0,96	880	917	898	0,43	1,72
	0,41	3,91	0,98	855	875			
	0,42	3,73	0,93	855	917			
1,7	0,42	3,88	0,97	865	892	883	0,41	1,63
	0,38	3,95	0,99	830	841			
	0,37	3,65	0,91	900	986			
1,6	0,37	3,76	0,94	910	968	948	0,37	1,47
	0,36	3,91	0,98	869	889			
	0,34	3,99	1,00	933	935			
1,5	0,31	4,01	1,00	930	928	925	0,32	1,27
	0,3	4,17	1,04	950	911			
	0,32	4,05	1,01	945	933			
1,4	0,28	4,4	1,10	1045	950	956	0,29	1,16
	0,27	4,67	1,17	1150	985			
	0,32	4,05	1,01	1026	1013			
1,3	0,32	4,38	1,10	1150	1050	1032	0,32	1,28
	0,32	4,12	1,03	1062	1031			
	0,28	4,1	1,03	1010	985			
1,2	0,25	4,2	1,05	1100	1048	1009	0,28	1,11
	0,3	4,1	1,03	1020	995			
	0,3	3,96	0,99	917	926			
1,1	0,29	4,11	1,03	1067	1038	993	0,30	1,19
	0,3	4	1,00	1014	1014			
	0,28	4,06	1,02	1030	1015			
1	0,25	4,1	1,03	1145	1117	1045	0,26	1,05
	0,26	4,07	1,02	1020	1002			
	0,25	4,1	1,03	1000	976			
0,9	0,24	4,25	1,06	1150	1082	1005	0,25	1,00
	0,26	4,1	1,03	980	956			
	0,25	4,4	1,10	1073	975			
0,8	0,22	4,7	1,18	1270	1081	981	0,24	0,96
	0,25	4,65	1,16	1030	886			
	0,3	5,1	1,28	1300	1020			
0,7	0,2	4,7	1,18	1500	1277	1134	0,23	0,93
	0,2	4,7	1,18	1300	1106			

Table 8: Results first experimental campaign brass, cutting speed 100m/min.

5.7 Lambda acual vs nominal

The true lambda value of each test was derived from the average of three chip thickness measurements, as the extruded chip thickness corresponds to the real shoe-tool gap. Knowing the feed, it is possible to get the true lambda, used to calculate the flow stress with the upper bound theory on which extrusion cutting is based.

5.8 Analysis of brass results

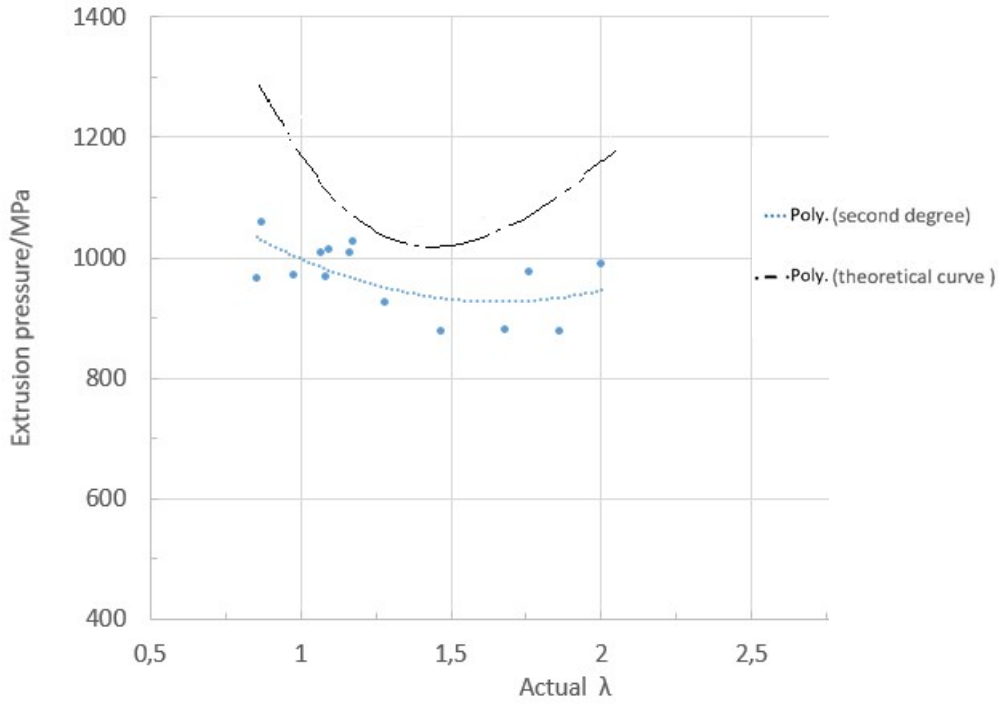

Figure 42: Extrusion pressure vs lambda for brass cutting speed 80m/min.

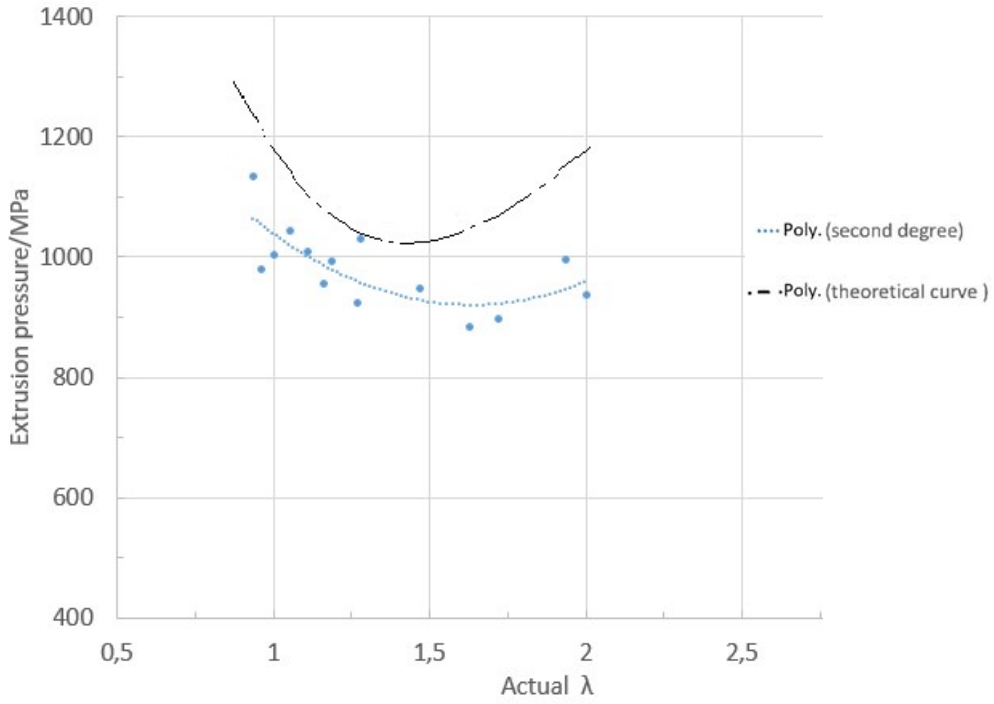

Figure 43: Extrusion pressure vs lambda for brass cutting speed 100m/min

The results obtained in the first experimental campaign on brass (Fig. 42), (Fig. 43) were not as desired, as the point of minimum pressure is at lambda equal to 1.5 and 1.9. Whereas to respect the theory of extrusion cutting it should have been reached this pressure in correspondence with lambda equal to 1.4 , and this is valid for both cutting speeds 80 and 100m/min.

From the graphs, it is possible to see that the experimental points are very scattered.

However, it is to note that the trend curve of the points is a second-degree polynomial, a parabola, and this is comparable with the theoretical curve of extrusion cutting. This was shown in the figure, which has the minimum point in lambda correspondence 1.4. and these two curves look similar, even if the trend curve has not the minimum at 1.4.

5.9 Influence cutting speed

The data obtained even if they do not have a minimum of extrusion pressure for lambda 1.4, are not completely to be considered useless, because overlapping the graphs obtained with cutting speed of 80m/min and 100m/min the points mix very

well. This means that cutting speed does not affect the process and this is a good thing because it allows us to eliminate one of the many variables.

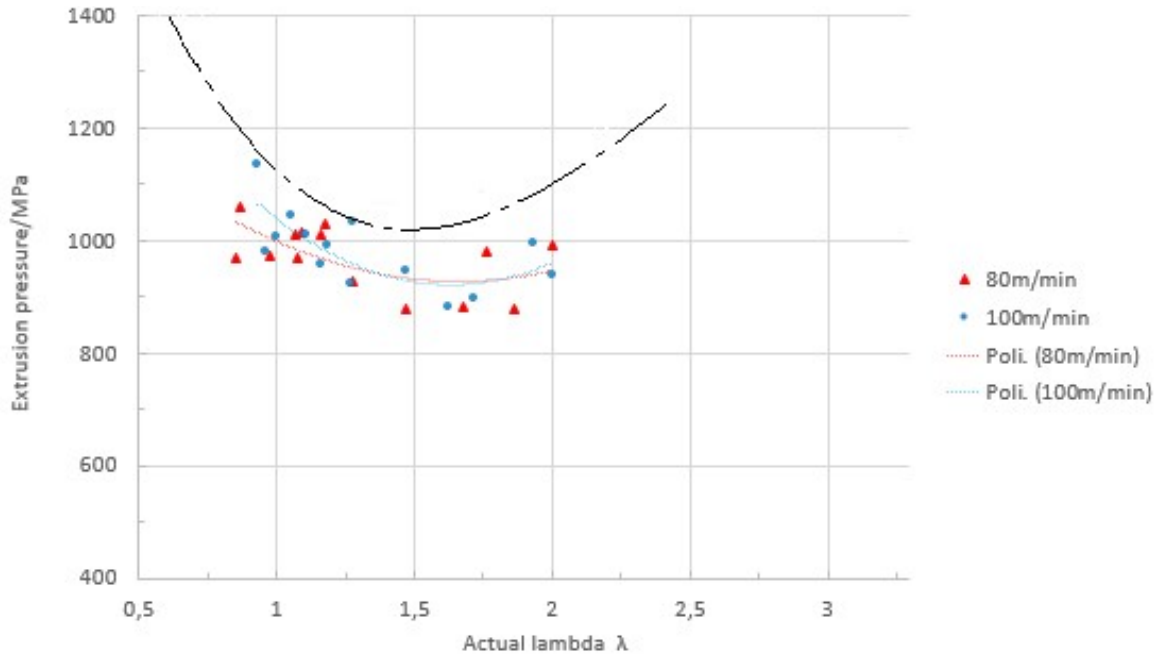

Figure 44: Overlapping the graphs obtained with cutting speed of 80m/min and 100m/min compared with theoretical curve

5.10 Problems in the first tests on brass

The crucial problem is that the point of least pressure is in correspondence with lambda 1.5 and 1.9 that is far from reflecting the theory which should be at 1.4. The dynamometer graphs are linear and clear (Table 9), but they have very high uncertainty. In addition, with very narrow lambda, which is from 1.4 to 0.8, the graphs have a bell shape, in the sense that the cutting force grows and then decreases, without ever finding process stability.

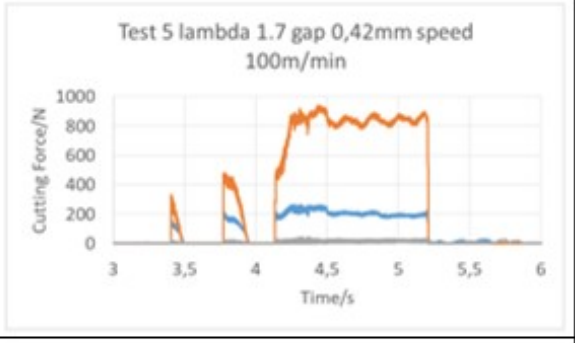	Here with lambda 1.7 which is not an "extreme" measure we can see a fairly linear trend of cutting force, obviously we must exclude the two signals of forces recorded before the real extrusion cutting process, maybe they are due to not perfect roundness of the disc.
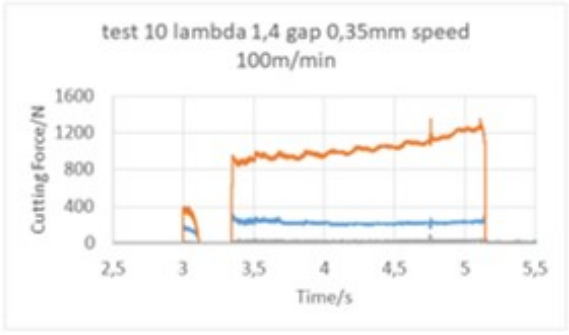	With lambda 1.4 it is possible to see the increasing force's trend is increasing, with a delta Newton from beginning extrusion to the end of extrusion about 300N and this is inadmissible. The process here is not stable.
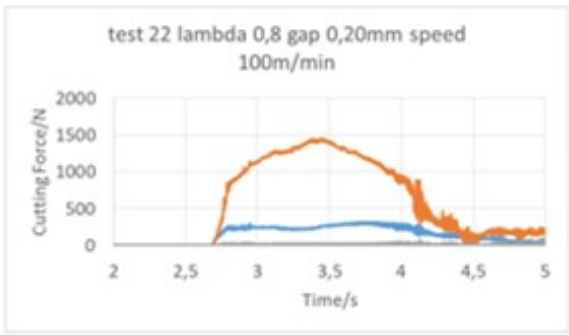	With lambda 0.8 the bell shape of the force is visible, and this is inadmissible! Especially since there is not an increase and a narrowing of such a width as to justify this trend

Table 9: Dynamometer graphs shape for brass.

With the first experimental campaign on brass, it is seen that the process is still not stable and robust, and it has to be found solutions to the problem:

• Point of minimum pressure not at 1.4.
• The graphics of the cutting force are not all linear, clear and stable.

5.11 Chip analysis copper

The copper tests were performed at 100m/min and 120m/min.

Starting with the thickness analysis, it was noted that there is a good agreement between the imposed gap and the measured chip thickness, except for very small gaps, where there is a deviation between the imposed and the real gap, perhaps due to the high pressure that is formed in small lambda.

Despite the changes made to the cutting parameters to solve the problem of widening, such as the increase of the rake angle and of the cutting speed that have been increased compared to the previous experiments, the workpiece widened a lot at the end of the run.

The widening creates a considerable difficulty in order to achieve a stable process, and even more to calculate the exact area of extrusion and even more to have a graph of linear forces.

Cutting speed 120m/min

Λ	S	thickness/mm	ave thickness/mm	*width*/mm	ave *width*/mm
		0,61		4,7	
2,5	0,625	0,61	0,61	5,1	4,87
		0,62		4,82	
		0,57		4,4	
2,2	0,55	0,55	0,56	5	4,95
		0,55		5,45	
		0,53		4,09	
2	0,5	0,52	0,52	4,08	4,13
		0,5		4,22	
		0,42		4,8	
1,8	0,45	0,4	0,45	5,5	5,49
		0,52		6,16	
		0,38		4,75	
1,6	0,4	0,36	0,38	5,49	5,46
		0,39		6,15	
		0,35		4,3	
1,4	0,35	0,35	0,37	4,6	4,65
		0,4		5,05	
		0,42		4,37	
1,3	0,325	0,4	0,41	5,1	4,72
		0,42		4,7	
		0,35		4,8	
1,2	0,3	0,36	0,37	5,3	5,37
		0,4		6	
		0,32		4,7	
1	0,25	0,36	0,35	4,87	4,96
		0,38		5,3	

Table 10: Chip-size analysis, highlighted by the average of chip's wide, every run was start at 3mm of workpiece's width.

5.12 Force analiysis copper

The graph of the forces is not linear, but has a growing trend certainly due to the progression of the width of the workpiece, which increases the extrusion force by increasing the extrusion area.

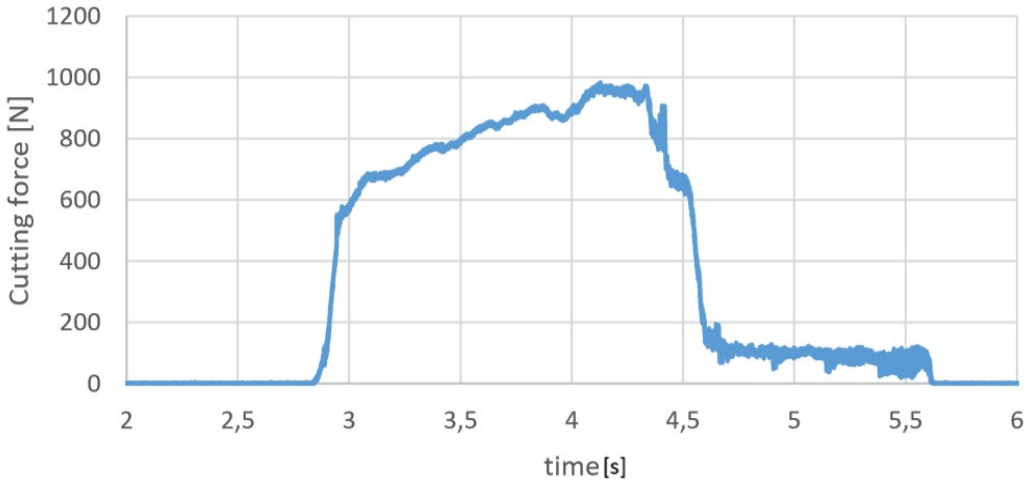

Figure 45: Copper force graph, extrusion cutting, lambda 1.6, cutting speed 120m/min.

This is a classic example of a cutting force chart that was recorded in experiments with copper (Fig 45).
For data analysis, as for brass, there were 3 different points in which the measurements of thickness, width and forces were taken, to try to bring the area of extrusion with the corresponding cutting force, going linearly increasing both.
The results obtained was very bad, as the error in the acquisition of force due to widening is too great, as can be seen in the (Fig. 45) in a run of 1.5 seconds of extrusion. The force increases from 600N to start of extrusion at 1000N of end of extrusion, with an increase, in this case, of 65% of the force required for extrusion. It can be seen that there is a too large inhomogeneity, which also affects the extrusion pressure-lambda graph.

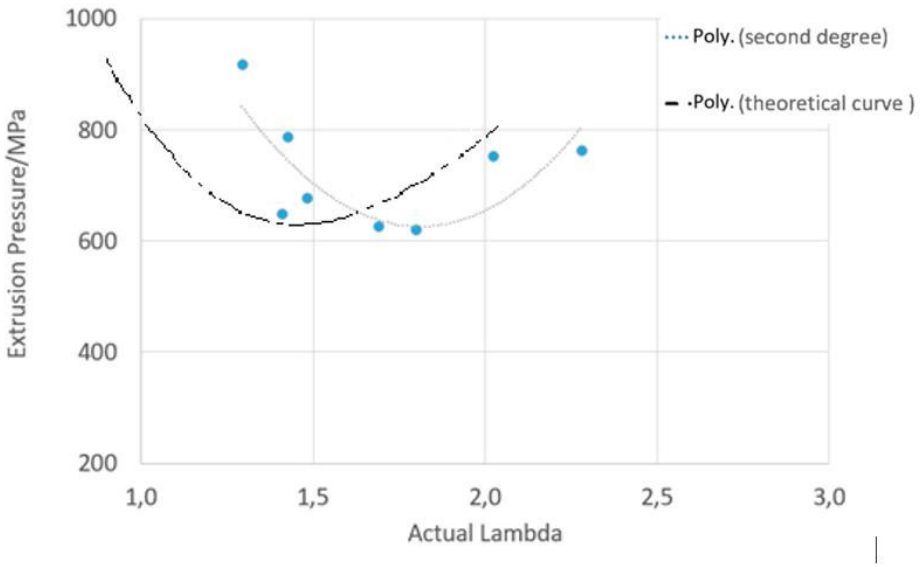

Figure 46: Copper, Extrusion pressure – Actual lambda, cutting speed 100m/min

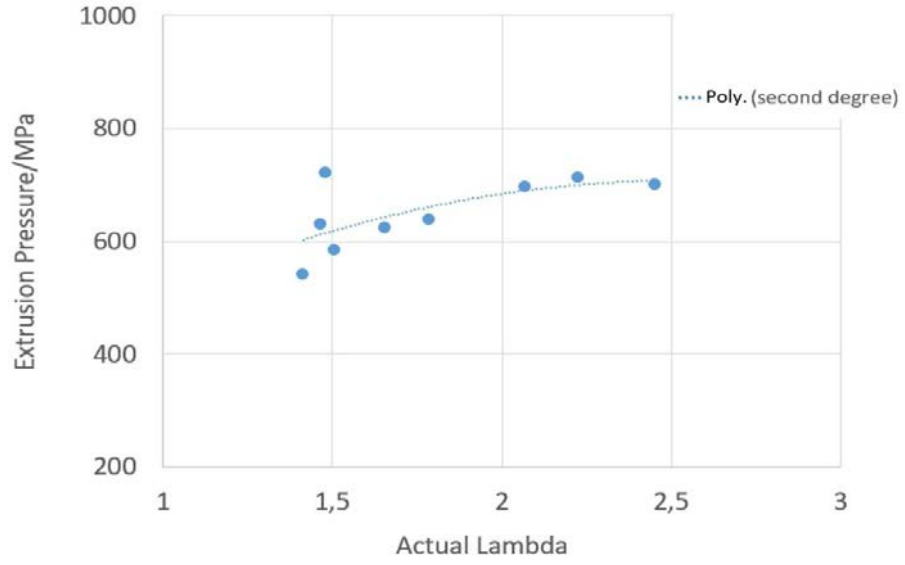

Figure 47: Copper, Extrusion pressure – Actual lambda, cutting speed 120m/min

5.13 Discussion of copper results

It is possible to see the results of the two test series in which the points are very scattered.

Studying the trend curve of the experimental data at 100m/min (Fig. 46), it is possible to see also that the fitting is by a second-degree polynomial curve, a parabola, exactly as the theory of extrusion cutting wants, having the minimum point at lambda 1.75. This value is in accordance with the value obtained from De Chiffre and Segalina [5] (Fig. 48) which found a minimum at lambda 1.84.

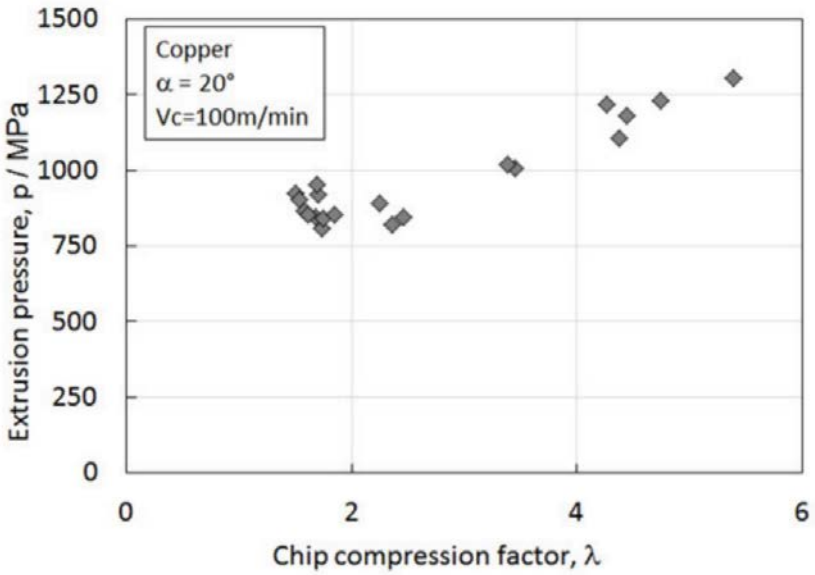

Figure 48: Copper's results [5]

The graph of the data obtained at 120m/min (Fig. 47) cannot be taken into consideration because the data are too few and scattered, both because of the graphs of the forces and because of the opening of the shoe.

As for brass, it is easy to see that there is no difference in the result in terms of extrusion pressure when the cutting speed changes, in fact here are found the data plotted in a single graph, which mixes perfectly.

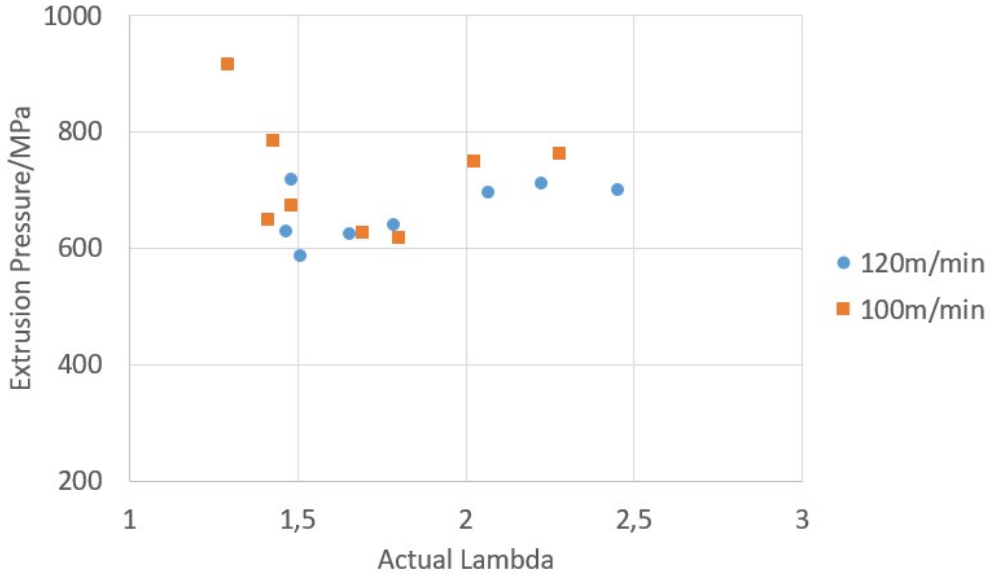

Figure 49: Copper, Extrusion pressure – Actual lambda, cutting speed 120m/min and 100m/min

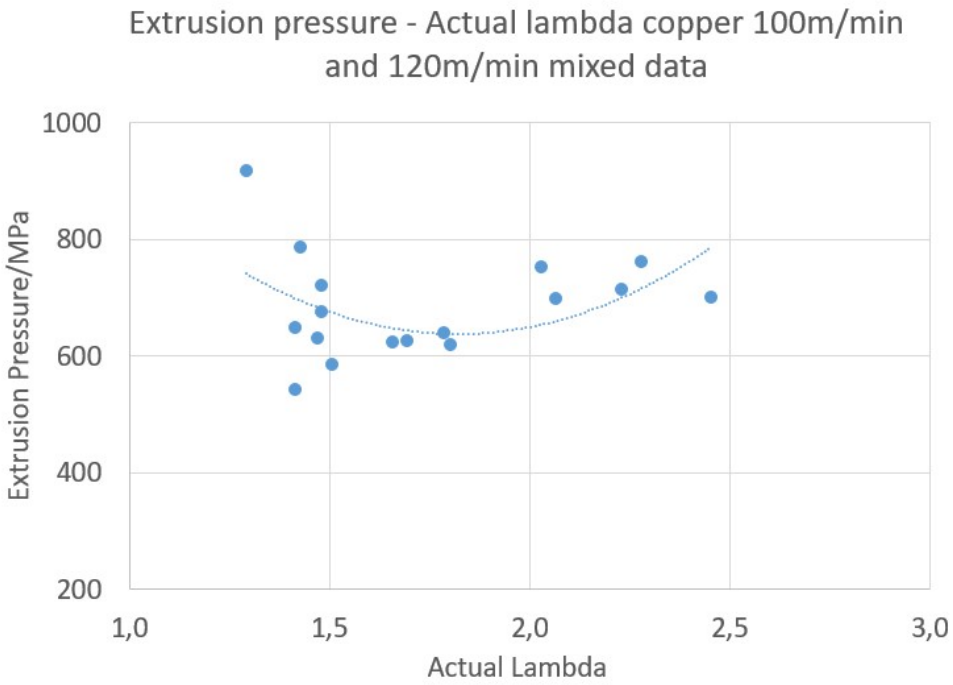

Figure 50: Copper, MIXED DATA, Extrusion pressure – Actual lambda, cutting speed 120m/min and 100m/min.

Analysing all the data obtained on copper (Fig. 49), (Fig. 50), ie both at 100m/min and at 120m/min, it is possible to note that a fitting second degree curve is always

present, with a minimum at lambda 1.8 confirming in part the validity of extrusion cutting.

5.14 Copper conclusions

In this thesis, with the changes made to the extrusion cutting process operating with copper, such as the increase in rake angle and in cutting speed, it was not reached the expected results, because the workpiece continued to expand, preventing the stability of the process.
Perhaps the cause of this problem is the high thermal softening that copper undergoes. A general analysis of the temperature in the extrusion cutting process is described below. Another cause can be the theory of the upper bound with a material such as copper, which is not entirely valid.

5.15 Aluminium test

In the few hours left available to the operator and the machine tool it was tested the extrusion cutting with aluminium.
It was tested tools with rake angles of 12°, 20° and 25°, different feed values and different cutting speeds, no combination led to the formation of a chip extruded from a stable process. As soon as the extrusion began, the workpiece-destroyed itself by expanding in an exaggerated manner (Fig. 51).

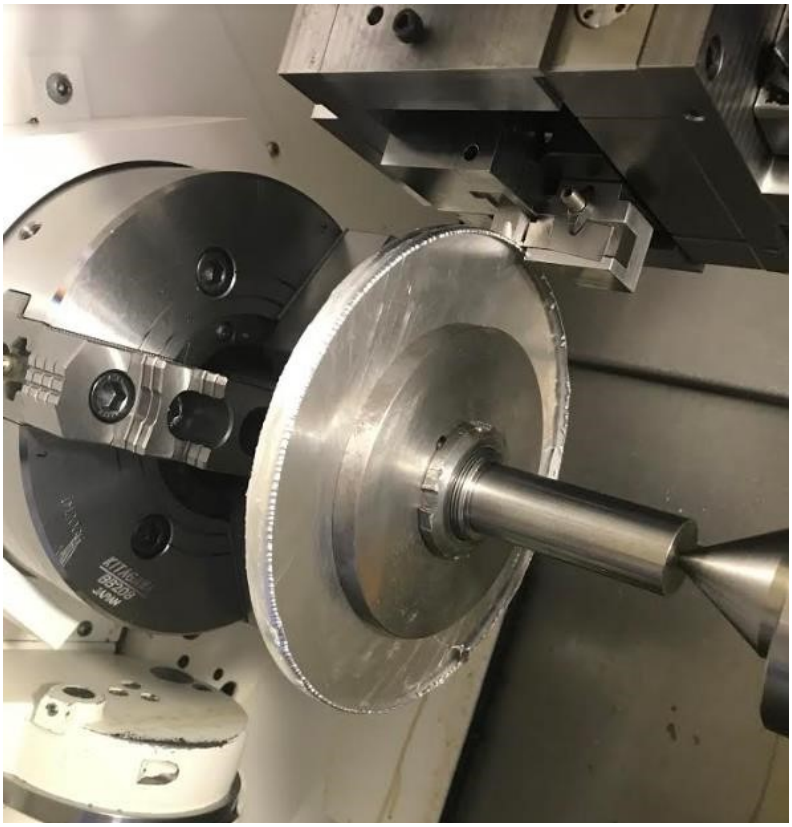

Figure 51: Aluminium workpiece destroyed

The conclusion is that the extrusion cutting process is currently not applicable to aluminium.

Chapter 6

6 Second experimental test campaign

In this chapter, it will be discussed the second campaign, which was carried out about one month after the first one, therefore there was time to see the results of the first campaign and to study possible solutions to the problems. This campaign is focused only on brass (Fig.52) and as with copper, the solutions adopted in the first campaign to avoid the widening have not yielded the desired results.

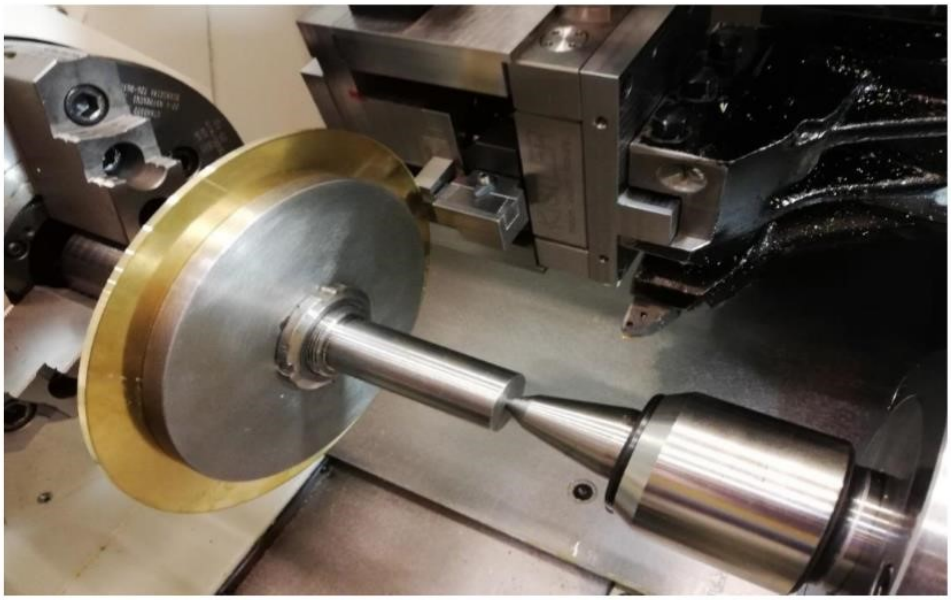

Figure 52: Photo of the second brass campaign.

6.1 Possible solutions for the new brass experimental campaign

A possible solution could be to extrude the material for a longer time in order to have a much flatter and longer graph of the forces.
Another solution was to precede the actual extrusion by an accompaniment of a cut with a feed of 0.1mm for 2 seconds, in order to stabilize the process and not have a strong and impulsive insertion of shoe-extrusion.
For the second experimental campaign, it was also thought to eliminate the problem of the data weight of the dynamometer file, which, as mentioned above, caused problems with Excel. Therefore, the z Force channel was eliminated and

the acquisition speed was decreased from the previous 20kHz to 5kHz in order to reduce the number of data to be plotted. However, there are already so many 5kHz because it means that a signal was recorded every 0.0002 seconds.
With the new test series, the lathe was no programmed for the extrusion on the mm removed on the disk diameter, but on the time of extrusion in order to have an extrusion for each run of 5 seconds and a first moment of turning / extrusion as accompaniment for 2 seconds with 0.1mm of feeds.
This is possible with an Excel worksheet (Tab.10) in which it is needed to know the cutting speed that will be constant for the experiment at 80m/min and the initial diameter of the workpiece. With this, it is possible to obtain the speed of rotation knowing the diameter, and what will be the final diameter knowing the speed and the constant feed equal to 0.25mm. Below it is attached an example excel worksheet that was used.

	Set-up Nr.	Rake angle [°]	Feed [mm/rev]	Cutting speed [m/min]	Cutting time [s]	WP Diameter [mm]	Spindle speed [rev/min]	Nr. Of rotation in cutting time	Tool displacement - Radial[mm]	WP Final Diameter [mm]
run1	1	12	0,10	80,00	2,00	210,00	121,32	4,04	0,40	209,19
	2	12	0,25	80,00	5,00	209,19	121,79	10,15	2,54	204,12
run2	3	12	0,10	80,00	2,00	204,12	124,82	4,16	0,42	203,28
	4	12	0,25	80,00	5,00	203,28	125,33	10,44	2,61	198,06
run3	5	12	0,10	80,00	2,00	198,06	128,63	4,29	0,43	197,20
	6	12	0,25	80,00	5,00	197,20	129,19	10,77	2,69	191,82
run4	7	12	0,10	80,00	2,00	191,82	132,82	4,43	0,44	190,94
	8	12	0,25	80,00	5,00	190,94	133,44	11,12	2,78	185,38
run5	9	12	0,10	80,00	4,40	185,38	137,44	10,08	1,01	183,36
	10	12	0,25	80,00	4,66	183,36	138,95	10,79	2,70	177,97
run6	11	12	0,10	80,00	4,91	177,97	143,16	11,73	1,17	175,62
	12	12	0,25	80,00	5,17	175,62	145,07	12,50	3,13	169,37
run7	13	12	0,10	80,00	5,43	169,37	150,43	13,61	1,36	166,65
	14	12	0,25	80,00	5,69	166,65	152,88	14,49	3,62	159,41
run8	15	12	0,10	80,00	5,94	159,41	159,83	15,83	1,58	156,24
	16	12	0,25	80,00	6,20	156,24	163,07	16,85	4,21	147,81
run9	17	12	0,10	80,00	6,46	147,81	172,36	18,55	1,85	144,10
	18	12	0,25	80,00	6,71	144,10	176,80	19,78	4,95	134,21
run10	19	12	0,10	80,00	6,97	134,21	189,83	22,06	2,21	129,80
	20	12	0,25	80,00	7,23	129,80	196,28	23,65	5,91	117,98

Table 11: Excel worksheet of cutting time and cutting speed.

During the second experimental campaign, it was also decided to perform a repeatability test, which was going to perform 5 tests in repetition with the same lambda value. This value was set at 1.4 because theoretically, it should have been the point of minimum pressure.

It was chosen lambda from 3 to 0.8 with steps of 0.2 in order to have a wide spectrum of data equally distributed. The lambda was chosen on the basis of the tool-shoe gap that was going to form, in order to have the gap equal to the size unitary of the thickness gauges available from the workshop. This was going to avoid corrections with 2 or even 3 thickness gauges one on the other and was going to reach the desired gap measurement. The aim was to eliminate possible errors made by operators, reduce uncertainty, simplify and increasing operation speed to the operator.

6.2 Setting second experimental test

The cutting speed for the second test was fixed at 80m/min. This was chosen because from the first tests it was seen that the cutting speed does not affect the extrusion pressure. The experimental points were, indeed, perfectly mixed between the 80m/min and 100m/min of cutting speed, and also the visual appearance of the chip was the same. Therefore, it was chosen 80m/min in order to preserve the tool from wear.

Every time that a new disk was mounted on the clamped, a run was made with the open shoe gap in order to achieve the roundness and eliminate any lobes that would have irreparably ruined the test having periodic peaks and valleys (Fig.53), without achieving stability of the process.

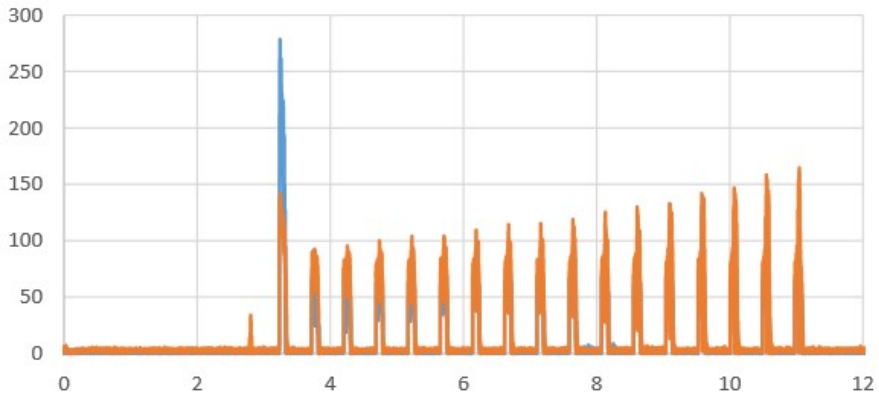

Figure 53: Force graph when does not proceed with restoring the roundness of the disk.

There were a lot of steel disks available in various sizes to sandwich the workpiece and in this way they were changed several times into small disks to avoid contact with the extrusion cutting equipment. Therefore, the roundness cleaning operation had to be done several times during the tests.
Also in this campaign, every chip produced was taken by the operator, left to cool and catalogued in a plastic bag with zip where had been previously noted the test number, the lambda used, and the gap that extruded the chip.
During the tests, there were no problems of any kind, not even noise and vibrations, only with very high lambdas was found a rolling of the extruded chip on the spindle (Fig.54), with the consequent breaking of the chip. The solution of inserting turned nylon cylinder on mandrel had been hypothesized to prevent the chips from rolling up the spindle, but it was experimentally seen that this behavior disappeared for lambdas from 2.2 to 0.8. so we not used any nylon cylinder.

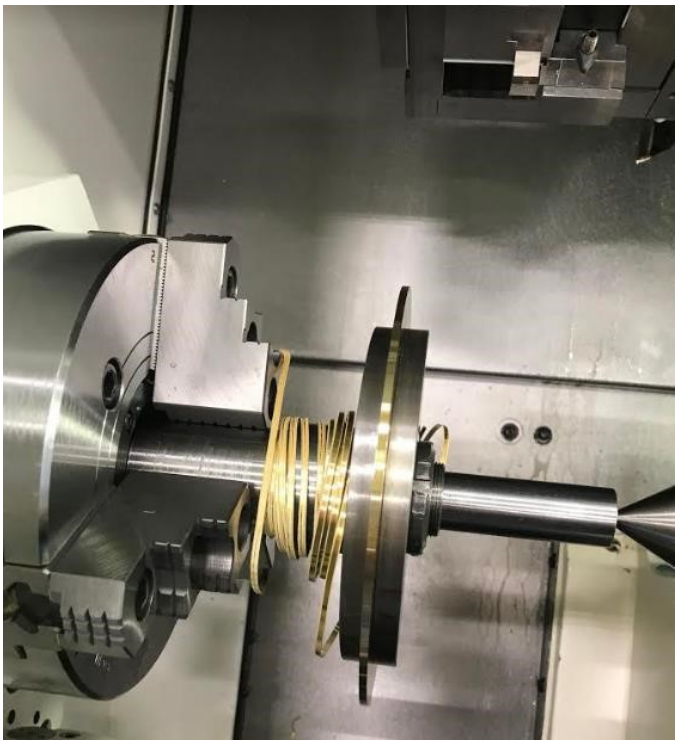

Figure 54: Rolling of the extruded chip on the spindle.

6.3 Force analysis

For the post-process, the excel program has always been used but with the second test, it was set the acquisition frequency of the dynamometer to "just" 5kHz the program. It was not crashed and after having eliminated two columns (true force and z force) the work was very fast.
In each graph, an adjustment work has been done on the axes, so as to display only the interested part after having identified the part of true extrusion (Fig.55).

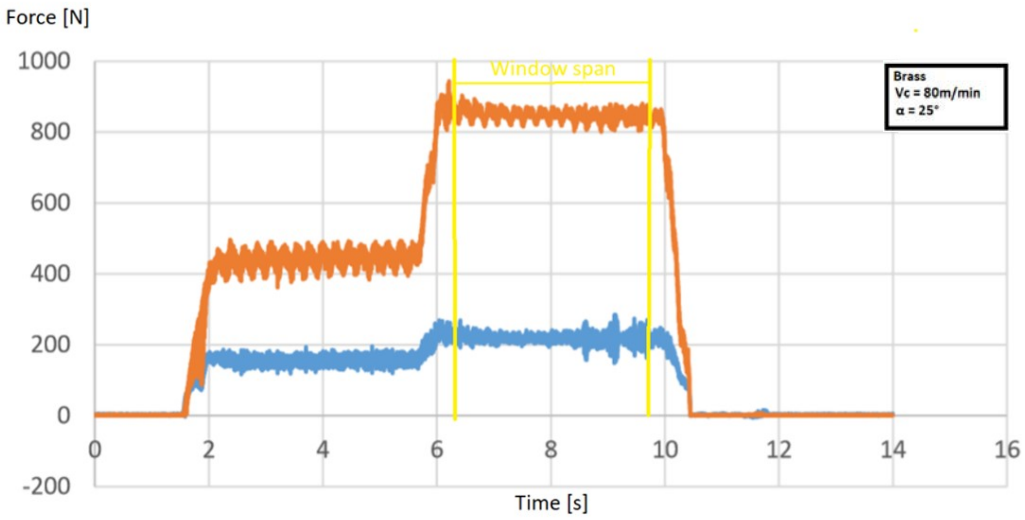

Figure 55: Typical graph of forces acquired in the second experimental campaign on brass with window span.

In fact the first part that can be noticed is the platoe where we have the cutting/extrusion with the feed 0.1mm and this part in not interested for this study. Instead the second part is about the real extrusion where the cutting force has been extracted. To do this, the lines of data describing the actual extrusion have been identified in the graph in window spam; 1000 lines at the beginning and 1000 at the end were eliminated, considering them as margin which are equivalent to about 5 percent of all the lines of the true extrusion. This is because the mathematical average of the force for each run was extracted to have the true strength without uncertainty due to reading.

6.4 Chips analysis

Each chip was extracted from the plastic bag, unwound along its entire length, which in the second test was very high compared to the first test. In the order of 2-5m and the chip width and thickness was taken in 3 distinct points 400-500mm after the extrusion "entry" area, in the middle of the extruded chip and finally at 400-500mm before the end.

With three thicknesses of three different zones of each chip, it was possible to analyse the constancy of the process. In this way, if it had been found that the thickness of the chip grew, decreased or varied during the extrusion, it would have meant that the process would not be stable. With the thicknesses obtained, it was satisfied as within the same run the thickness was constant with a variation of a few cents of millimetres that could be considered irrelevant.

The second control step consisted in the comparison between the imposed gap, and the chip thickness that should be exactly the same since the gap represents the area of the extrusion matrix, net of small elastic deformations that can occur at the exit from the extrusion die.

From this control, it can be seen that the lambda 2.6, 2.6 and 2.2 have extruded chip thicknesses that are clearly larger than the gap measurement (Tab.11).

Here it is not to take the average of the pressures as in the first campaign in which the force graph is linear and constant.

Imposed Λ	t [mm]	w [mm]	area [mm^2]	Fc [N]	P [MPa]	Ave t [mm]	actual λ
	0,76	3,3					
3	0,77	3,35	0,83	935	1130	0,76	3,04
	0,75	3,28					
	0,75	3,32					
2,8	0,76	3,34	0,83	920	1106	0,75	3,00
	0,73	3,32					
	0,74	3,34					
2,6	0,76	3,4	0,85	905	1071	0,76	3,04
	0,77	3,4					
	0,6	3,27					
2,4	0,6	3,25	0,82	853	1042	0,60	2,04
	0,6	3,3					
	0,75	3,3					
2,2	0,7	3,28	0,83	900	1088	0,70	2,80
	0,65	3,35					
	0,72	3,28					
2,2	0,73	3,3	0,83	910	1103	0,72	2,88
	0,72	3,32					
	0,52	3,28					
2	0,55	3,3	0,82	830	1012	0,53	2,12
	0,51	3,26					
	0,55	3,3					
2	0,52	3,35	0,83	830	1001	0,53	2,12
	0,52	3,3					
	0,45	3,29					
1,8	0,46	3,3	0,82	817,5	998	0,46	1,84
	0,47	3,24					
	0,42	3,29					
1,6	0,41	3,4	0,84	832,5	992	0,42	1,68
	0,42	3,38					
	0,42	3,41					
1,6	0,44	3,4	0,84	842,5	1003	0,43	1,72
	0,42	3,27					

Table 12: Analysis chip brass second campaign.

Imposed Λ	t [mm]	w [mm]	area [mm^2]	Fc [N]	P [MPa]	Ave t [mm]	actual λ
	0,36	3,29					
1,4	0,37	3,45	0,85	875	1030	0,36	1,44
	0,36	3,45					
	0,38	3,34					
1,4	0,36	3,46	0,85	875	1026	0,37	1,48
	0,37	3,43					
	0,35	3,48					
1,4	0,37	3,47	0,87	880	1013	0,35	1,40
	0,34	3,47					
	0,35	3,45					
1,4	0,37	3,44	0,86	880	1020	0,36	1,44
	0,35	3,46					
	0,32	3,65					
1,2	0,33	3,64	0,92	935	1021	0,33	1,32
	0,34	3,7					
	0,31	3,52					
1,2	0,32	3,58	0,89	940	1054	0,31	1,24
	0,31	3,6					
	0,28	3,71					
1	0,27	3,81	0,95	1005	1059	0,28	1,12
	0,3	3,87					
	0,27	3,84					
1	0,3	3,82	0,96	1020	1066	0,29	1,16
	0,3	3,82					
	0,24	3,9					
0,8	0,22	4,1	1,02	1225	1200	0,23	0,92
	0,24	4,25					
	0,75	3,2					
open	0,76	3,2	0,81	950	1172	0,75	3
	0,74	3,33					

Table 13: Analysis chip brass second campaign.

This problem is most likely due to an error on the part of the operator who did not close the shoe holder on the gap required for the specific run with the necessary force and therefore when the extrusion process started it was already opened by great pressure.

These runs with this anomaly are to be treated as an outliner and cannot be used as reliable data and are plotted in red triangles to indicate to the reader what they are.

6.5 Repeatability test

A repeatability test was made to test whether the process was repeatable and stable.

Repeatability is the degree of agreement between a series of measurements of the same measurand, when the single measurements are made leaving the measurement conditions unchanged. In particular, the measures must comply with the following conditions:

• the same measurement method must be maintained;
• must be carried out by the same operator;
• must be carried out with the same measuring instrument;
• must be made in the same place;
• must be carried out with the same conditions of use of the instrument and the measurand;
• must be carried out in a short period.

Repeatability should not be confused with reproducibility, which evaluates the consistency of measurement results by varying one or more measurement conditions.
The presence of discrepancies at the same measurement conditions highlights the existence of random error sources that makes the process not robust. The latter are a natural effect of the practical impossibility of perfectly controlling all the infinite sources of influence. It is fundamental, in practice, that the discrepancies are not so wide as to make the measure not significant. The assessment of repeatability is therefore fundamental in defining the precision of the measurement.

It has been decided to make 5 runs in succession with lambda set to 1.4, as according to De Chiffre's theory and experiments [1], in order to obtain the most beautiful chip and the less extrusion pressure necessary. Given that in the first

experimental campaign there was a difficulty in identifying the minimum point, with 5 data instead of one it should be easier to identify it.

6.5.1 Results repeatability test

Imposed Lamda	Imposed gap/mm	Ave Width/mm	Ave Thickness/mm	Actual Lambda	Cutting Force/N	Extrusion pressure/Mpa
1,4	0,35	3,40	0,36	1,44	875	1030
1,4	0,35	3,41	0,37	1,48	875	1026
1,4	0,35	3,47	0,35	1,40	880	1013
1,4	0,35	3,45	0,36	1,44	880	1020

Table 14: Results repeatability test

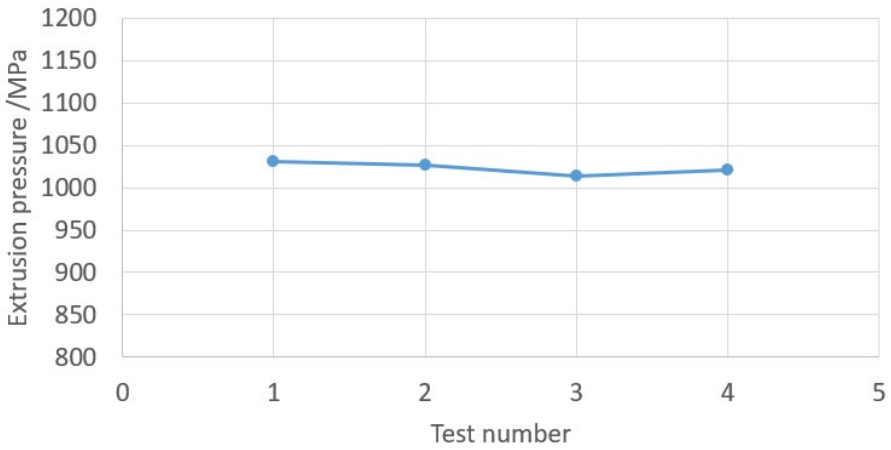

Figure 56: Extrusion pressure on each test

5 runs were performed, but in one of these there was an acquisition error and therefore it cannot be considered valid.

6.5.2 Conclusion repeatability test

Analysing the 4 valid tests, it can be noticed that there is excellent repeatability (Fig.56), with variations of a few hundredths of a millimeter on the width and just some Newton on the force (Tab.12), but in percentage, these errors are very low, in the order of 1%. Thus, it can be concluded that the process is repeatable.

It would have been very interesting to see a linear lowering of the forces between one run and the other, which would have meant that an increase in temperature of the workpiece would cause a slight thermal softening that would affect the force required for extrusion. Nevertheless, the test execution mode takes about 4

minutes between each test, which gives the workpiece the time needed to cool it down, bringing the surface temperature back to around room temperature, invalidating this search for thermal softening.

6.6 Discussion of results

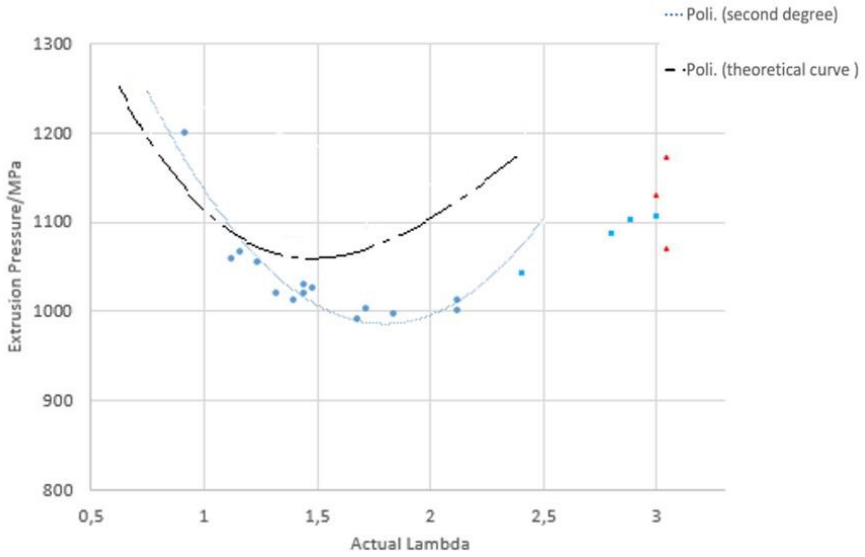

Figure 57: Extrusion pressure vs real lambda graph, second brass experimental campaign.

Here it can be seen that the theorized curve of the upper bound model is present. Moreover, it is possible to see that there is a parabolic curve that has a minimum and this is the extrusion curve in which there is the real extrusion. It has a minimum for 1.68, not yet 1.4 as the theory would suggest, but certainly better than the first experimental campaign where the point of minimum pressure was resulted for lambda 1.5 and 1.9.

Then, there should be a horizontal straight line that starts from lambda 2.4 up to over 3 which represents the linearity pressure that is necessary for classical turning; in the graph these points are indicated by blue square. This straight line, however, is difficult to notice because it must have been formed by precise points, which are out liner that distorts the linearity. The outliners are due to an opening of the shoe.

The solution to keep the extrusion time longer was excellent, as now the process is very stable, and even with reduced lambda, the graphs of the forces no longer present the bell-shaped trend.

However, it is still difficult to find a perfect commonality with the theory, it should modify the mathematical model of the upper bound model.

6.6.1 More abstract discussion

A different discussion can be made if it is considered that the value of h may be affected by a systematic error. In fact in all the results analysis made, the value of h was considered as constant, and it was perfectly set by the operator at the beginning of the session test on the value of 0.25mm. However, from the analysis of the thickness, it was compared with the value of the set gap and it was always seen a discrepancy (Fig. 57).

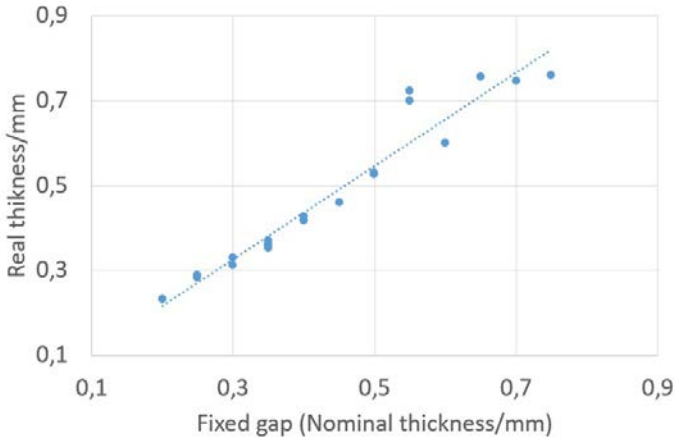

Figure 58: Deviation from the set value of gap shoe-tool and real gap shoe-tool.

Therefore, it may arise that the value of h, is not really 0.25mm but a little greater. However this could not be verified due to lack of time. Assuming that the value of h had been 0.28mm instead of 0.25mm, the real lambda values would go down and the entire extrusion pressure vs real lambda curve would shift towards smaller values, approaching the values of the theory of extrusion cutting (Fig.58). In fact a minimum point equal to lambda 1.5 would be reached, which is very close to that reached by De Chiffre and Segalina [5], confirming that the theory extrusion cutting is robust.

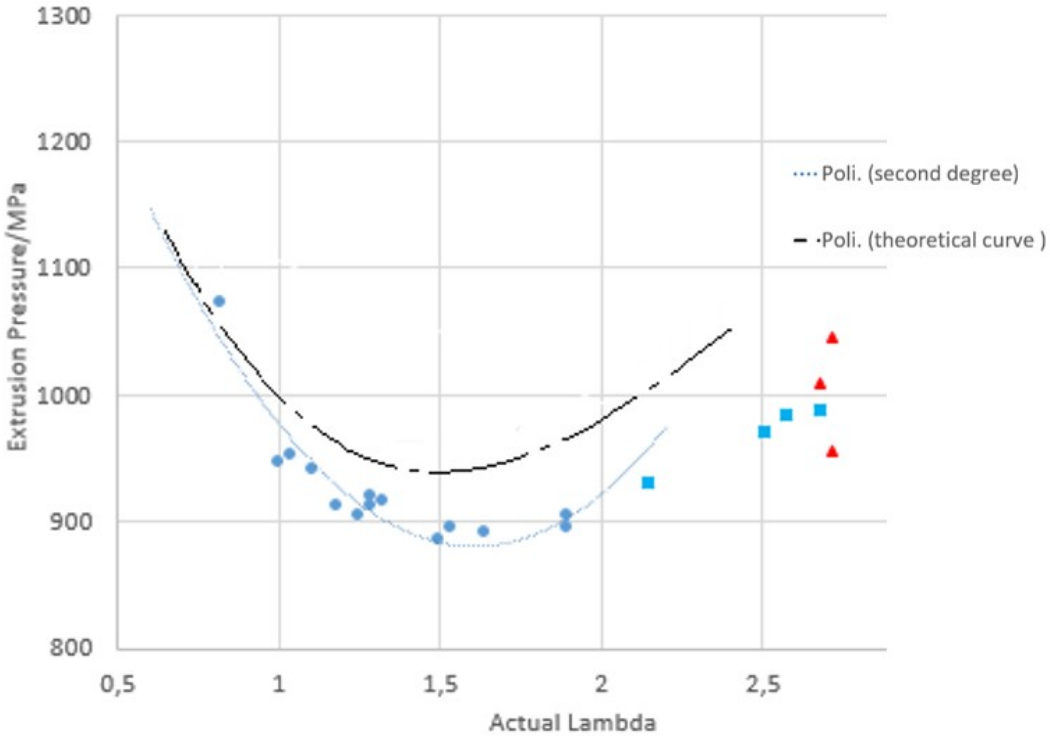

Figure 59: Extrusion pressure vs real lambda graph, second brass experimental campaign if there was a error to setting feed.

6.7 Other graphs

The graph that says if the experimental data respect the theory of extrusion cutting is the extrusion pressure in function of lambda, having a second-degree interpolation curve with a minimum close to lambda 1.4 as already explained. However, it is possible to obtain graphs in the function of lambda also for the strain, strain rate, temperature, and flow stress. (Fig.59,60,61,62)

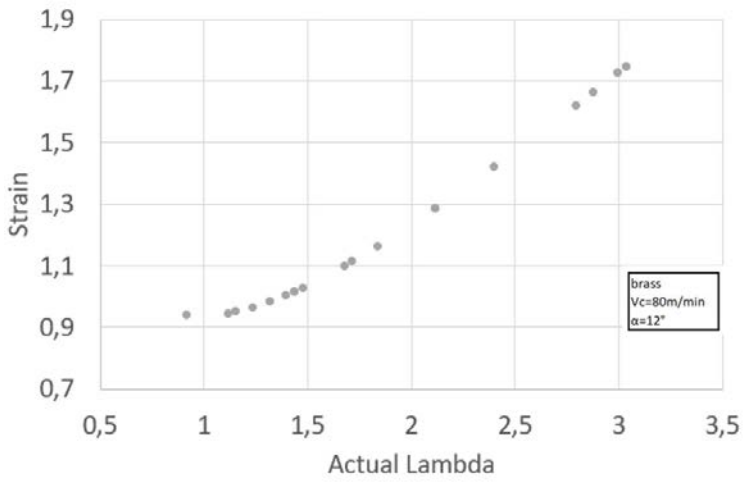

Figure 60: Equivalent strain as function of chip compression factor

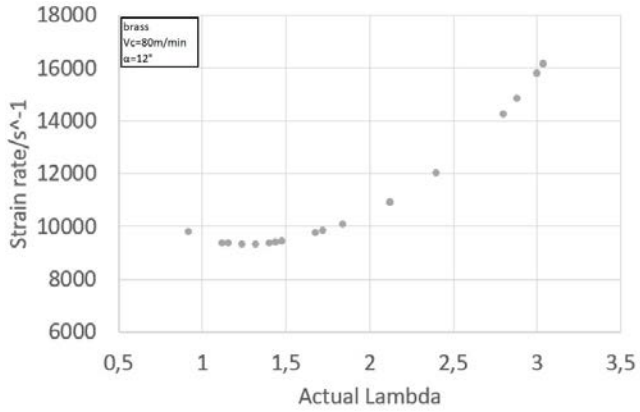

Figure 61: Equivalent strain-rate as function of chip compression factor.

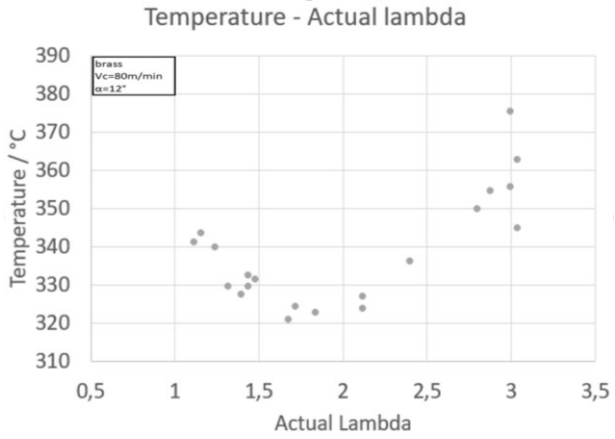

Figure 62: Cutting temperature as function of chip compression factor

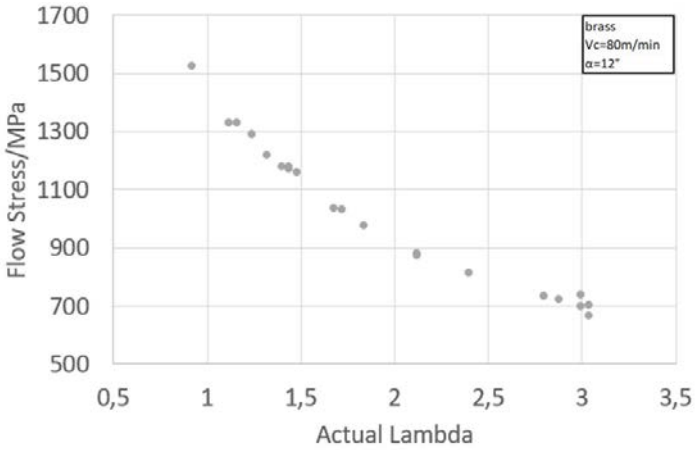

Figure 63: Equivalent stress as function of chip compression factor.

These graphs would be fundamental to interpolate a 4D function (Fig.63) and derive a constitutive equation as Segalina did in collaboration with the IT department, but in this thesis it will not be derived.

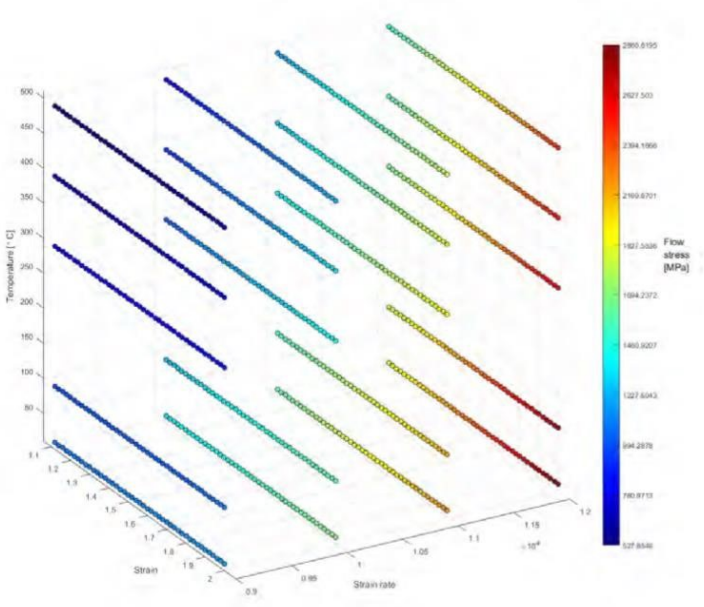

.

Figure 64: 4D Plot function of strain, strain rate, temperature and stress, Segalina 2016

6.8 Comparison of historical data

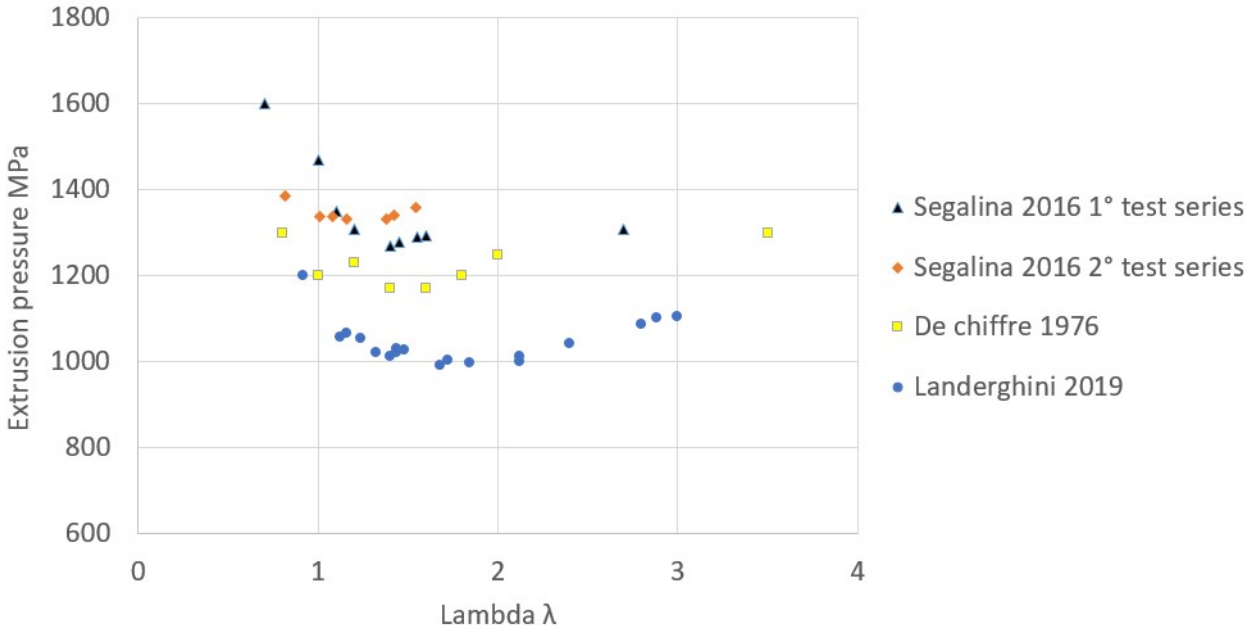

Figure 65: Graph that collects all historical data of extrusion cutting with brass

All the historical data of extrusion cutting made by extruding brass have been plotted in the graph (Fig.64). It means those from the first tests obtained by De Chiffre in 1976 [1], when he theorized extrusion cutting, until Landerghini 2019 (this work) results with new equipment, passing by the results of Segalina [3]. Even Astrup [4] had achieved results, but having made experimental mistakes, and having had some technical problems, they are not reliable and therefore were not included.

The data of Landerghini 2019 show lower extrusion pressure than those obtained by De Chiffre [1] in 1976. It could be due to a no optimal dynamometer type equipment, or due to the extrusion cutting equipment, or due to a different composition of the extruded brass. However, the difference is about 150N and it corresponds to a 10-15% error that is acceptable. This means that here is a difference of just 15kg of force necessary for the extrusion. In addition, it is possible to see an agreement in the minimum curve, which is a very comforting result.

Segalina's data [3], on the other hand, achieve a higher extrusion pressure than that used in this work. This is because he made the mistake obtaining the

extrusion pressure by dividing the cutting force always in the same area, not considering the modest widening of the disk, which is valid also for the brass.
In conclusion, it can be stated that there is repeatability in the process because the historical data obtained with different equipment mix well.

Chapter 7

7 Slip line method

It was seen from the experimental data that the point of least pressure was not exactly at lambda 1.4 as the theory of the upper bound suggests, so it can mean that it can be used a mathematical model on which extrusion cutting is based as a process to derive the behavior of the material, alias constitutive equations, being supported by a vast amount of data obtained from experimental tests.

7.1 Matlab as generator of true slip line field

With the Matlab software and a program developed by professor Chris Valentin Nielsen in Matlab that draw the slip line field, the variables that can be changed, are:

- The rake angle value;
- The theta which is the value of the angle formed by slip line fan, the value of theta is strictly connected to the value of lambda or more precisely to the shoe-tool gap;
- Friction factor used in place of the coefficient of friction. Eq. 2.3 which can vary from 0 to 1, with 1 considered sticking, that is, the material sticks and the new material flows on the one attached, in this case we used a value of m = 1 and m = 0.8 which means that the material flows on the rake angle with friction, but does not stick.

By changing only these variables, the program returns images of the slip lines and the corresponding lambda value.
The purpose of obtaining these images of slip line fields was, first of all, to understand to what level of lambda the theory on which extrusion cutting is based can be considered valid, ie the "simple upper bound model" and subsequently try

to obtain an upgrade of the simple mathematical model to find a major agreement with the experimental data.

In fact, the theory of extrusion cutting developed by Professor De Chiffre [1], hypothesizes only a line of discontinuity and another small line on the rake angle which is valid for a normal cutting without extrusion.

With the images obtained it will be possible to see how much it is deviated from the theory of the upper bound using a slip line method that gives a true solution.

Several tests were performed (Fig.65) with different combinations:

- Varying m, from 0.8 to 1
- And varying lambda, from 1, 1.4, 1.8

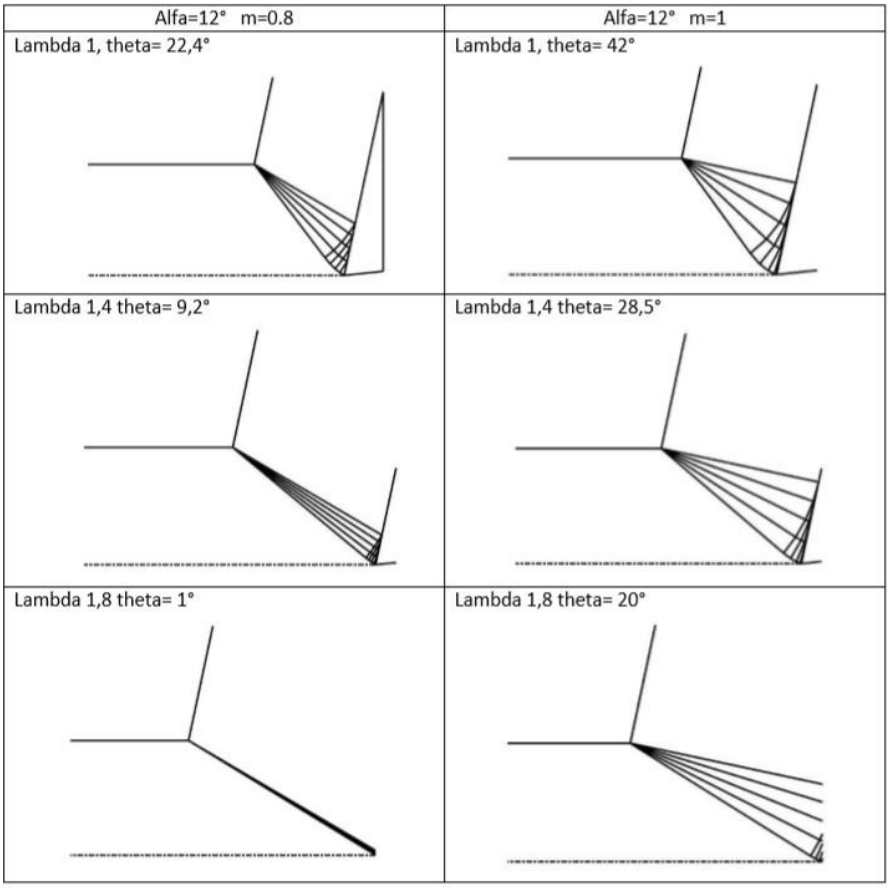

Figure 66: Extrusion cutting slip line field from Matlab program

From the table, it can be deduced that with $\Lambda = 1.8$ it still has a linear slip line, practically without a slip line fan. A great indication that the theory of extrusion cutting is valid up to $\Lambda = 1.8$ and m = 0.8 but this is not completely correct to say, because the theory is based on strong simplifying assumptions example that m is equal to 1.

It can be noted that if we keep increasing the lambda value for example 2.2 with m = 0.8 the slip line field becomes negative, that is the theta gets negative, and this is physically impossible. Therefore, it can be affirmed that the program developed on Matlab to describe the slip lines has a validity limit, as long as the slip line becomes singular (Fig.66).

This acceptability limit phenomenon is more pronounced for m = 0.8, while for m = 1 this phenomenon does not occur yet for a lambda value as high as 3.

This fact suggests that the true value of m will certainly be between 0.8 and 1.

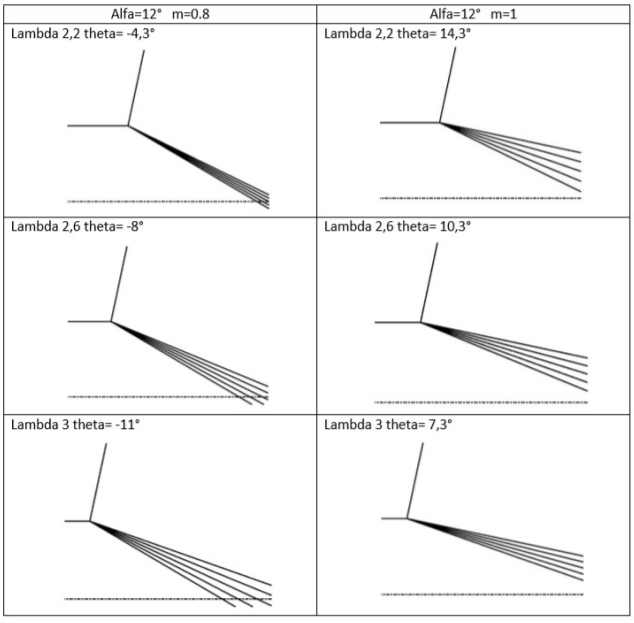

Figure 67: Singularity of Matlab program

7.1.1 Determination m "real"

The next step that has been done is to try to understand through the Matlab program, which is the friction factor m, the most truthful in our experiments, given that m = 0.8 and m = 1 were assumptions based on theoretical experience

for which are reasonably permissible values in cutting. To do this, it was used an iterative method as opposed to how was got the previous graphs.
First of all it needs to know the natural chip compression, which has been experimentally obtained through an orthogonal free turning, without the restriction of the shoe, using the same tool used for extrusion cutting and with the same rake angle. The chip compression is closely related to the type of material and to the rake angle used, in the case of brass and rake angle of 12°, the "natural" chip compression is 2.9 derived from chip thickness divided by feed.
Knowing that in normal turning, there is only one line of discontinuity, in the Matlab program it was inserted the rake angle 12° as a fixed parameter and in an iterative way, it was entered the values of theta in order to obtain a single line of discontinuity at lambda 2.9 obtaining a m equal to 0.92.

7.2 Modification Mathematical model based on slip lines

The theoretical formulation of extrusion cutting as a process to derive p/k and therefore a material constitutive equation, derived from De Chiffre 1976 [1], is based on the upper bound model.

7.2.1 The upper-bound

The upper-bound theorem states that any estimate of the collapse load of a body made by equating the rate of internal energy dissipation to the external forces will be equal or be greater than the correct load.
The analysis involves:

1. Assuming an internal flow field that will produce the shape change.
2. Calculating the rate at which energy is consumed by this flow field.
3. Calculating the external force by equating the rate of external work with the rate of internal energy consumption.

The flow field can be checked for consistency with a velocity vector diagram or hodograph. In applying the upper bound model to metal-working operations, several simplifying assumption are invoked:

1. The material is homogeneous and isotropic.
2. There is no strain hardening.
3. Interfaces are either frictionless or sticking friction prevails.
4. Usually only two-dimensional (plane-strain) cases a reconsidered with deformation occurring by shear on a few discrete planes. Moreover the material is rigid.

With a lot of experimental test data, it was seen that it deviate a bit from the theory, in fact in point of minimum pressure it is found a little above lambda 1.4. This is almost certainly due to the many, perhaps too many, assumptions that have been made to derive p / k using the upper bound method. In fact, the upper bound is valid in free turning, but when it was extruded the slip lines changed completely, and that is when the shoe-tool gap tightens so as to start the extrusion, that with the starting parameters (brass and 12° of rake angle) starts at lambda 2.9, the model cannot be considered valid enough to describe the process.
With Professor Chris Valentin Nielsen's program, it was possible to eliminate some of these simplifications, used for the upper bound, using the slip line theory. In this way, it is possible to work on a field of discontinuity more similar to reality [14].

7.2.2 Slip line

The theoretical foundation of the slip line method starts from Coulomb in 1773, then Rankine in 1857, then Levy in 1873. The method was definitively established by Hencky in 1923 and Geiringer in 1930, deriving equations to solve the field of tensors and velocity, then Prager in 1951 introduced the hodograph, and Hill described the extrusion slip line fields.
The goal of the slip lines is to describe the plastic deformation of solids subjected to stress.
The solution found with this method will be a complete solution, using simultaneously the field of tensors and velocities (deformations).

Slip-line field theory is based on study of a deformation field that is both geometrically self-consistent and statically admissible. Slip lines are planes of maximum shear stress and are therefore oriented at 45◦ to the axes of principal stress. Basic assumptions are:

1. The material is isotropic and homogeneous.
2. The material is rigid-ideally plastic (i.e. no strain hardening).
3. Effects of temperature and strain rate are ignored.
4. Plane-strain deformation.
5. The shear stresses at interfaces are constant, usually frictionless or sticking friction.

The advantage of using the slip line method which yields an "exact" power compared to the upper bound that with which greater power is obtained than the real one.

The explanation of the method will not be included in this thesis, as it is complex and tedious for the reader, see Hill's books [13].

7.2.3 Equal-channel angular extrusion

This extrusion method is very similar to extrusion cutting, except that there is no area variation and the material is enclosed on all sides by the matrix, which creates friction from multiple fronts. The slip line field is also very similar.

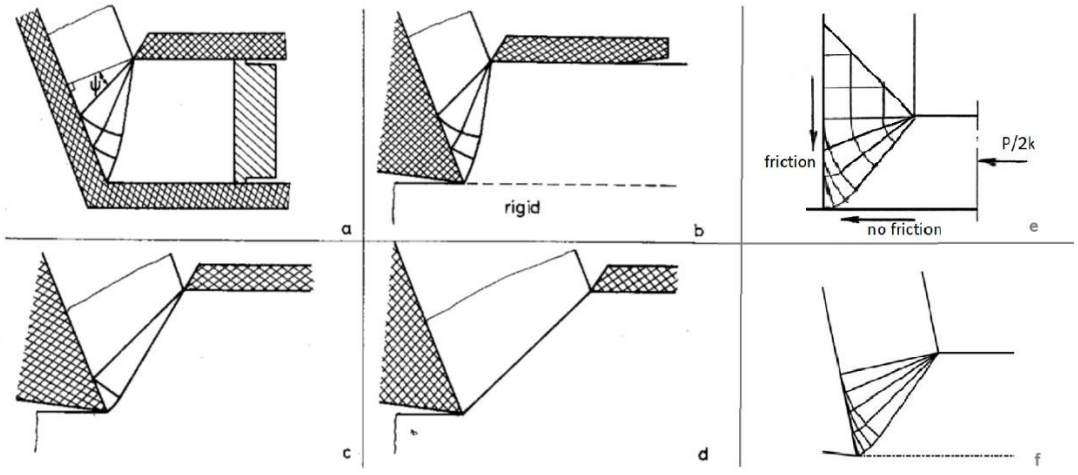

Figure 68: Analogy between extrusion-cutting, side-extrusion and ECAE.

(a) plane side-extrusion with inclined bottom wall, (b) extrusion-cutting with a large deformation zone, (c) extrusion-cutting with narrow deformation zone, (d) theoretical limit of extrusion-cutting, (e) slip line field analogy with ECAE process with no friction in one channel, (f) slip line field extrusion-cutting from Matlab.

In the sketches it is possible to observe the analogy between side extrusion process with the relative slip line, the extrusion cutting with the corresponding slip line field by De Chiffre 1976 [1], and figure (f) which is the slip line field obtained with the program Matlab, which, seeing its perfect harmony with the field obtained from [1], it confirms that it was right the field of [1]. And the analogy of field of slip line with a process known as equal-channel angular extrusion (ECAE) by V.M.Segal it was discovered in the 70s [15] in the URSS, and therefore it was "hidden" from the scientific community, which was born as a method for reduction of the size of the metal grain. There have been many studies on this process these days, so it is a help to go into an in-depth study of a future thesis or Ph.D. on the subject, as an aid to extrapolate the p/k or p/2k equation based on the slip line field and not on the upper bound model.
It was possible to derive p/k knowing the pressure at a point. Although the method is simple, it is required to take in consideration different parameters and a multitude of trigonometric relationships. Thus, it would be of interest to be investigated during a Ph.D. project.

Chapter 8

8 Extrusion cutting temperature study

An attempt to take temperature into account, in the theoretical model of extrusion cutting.

8.1 Introduction to temperature study

Temperature analysis is very important for determining the constitutive equations of the material because with the temperature the metal behavior change. If the temperature increases in the metal, the flow stress-strain curves will go lower, going to make the metal less hard and more ductile, up to the cases at the limit of reaching the melting point where the metal becomes viscous liquid.

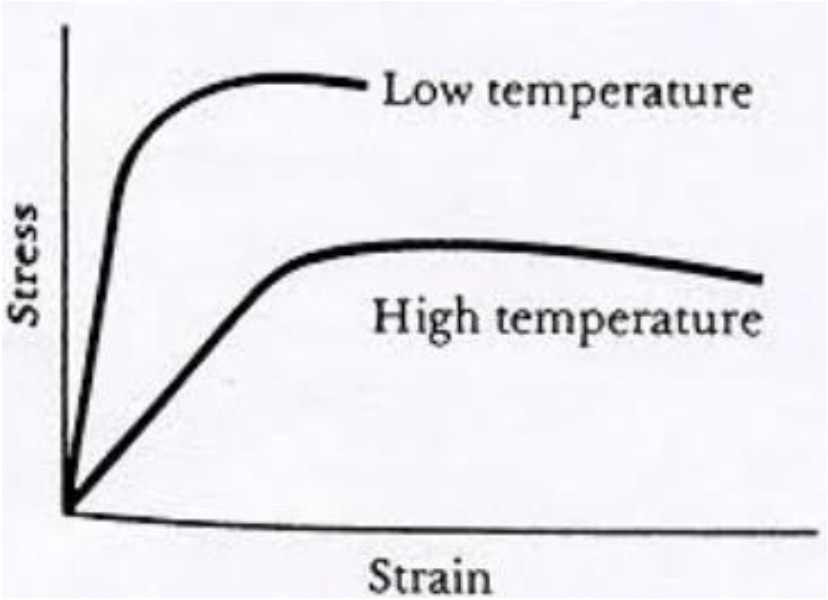

Figure 69: Strain-stress curve of general metal changing with temperature.

This effect should reduce the forces needed for extrusion, or turning or all the mechanical processes that rely on plastic deformation.

Then there is the effect of thermal softening, the local increase in temperature can result in softening that leads to localization. In the extreme case, these bands are

called adiabatic shear bands. Regardless of the initial softening mechanism, the localized deformation leads to an acceleration of strain rate. Eventually, there is heat concentration and thermal effects in most situations. There are several excellent reviews available in the literature. Review articles by Rogers (1979), Stelly and Dormeval (1986).

To do the opposite work, there is the strain hardening or called also work hardening is a metallurgical phenomenon whereby a metal material is strengthened two to plastic deformation.

In metallic solids, plastic deformation is caused, at a microscopic level, by latex defects called dislocations, which facilitates the sliding of the crystalline planes moving through the material. Ending up interfering with each other, blocking each other, increasing the point defects and thus increasing the mechanical resistance It must be added that the dislocations in movement accumulated against the grain boundaries (which are barriers to the motion of dislocations), causing them to break. The result of this deformation of the crystalline grains and their lengthening in the direction of the effort.

8.2 Effects on mechanical properties

Increase the yield stress and hardness, the properties of ductility (such as elongation and striction) and static and dynamic tenacity (such as resilience) diminish.

In extrusion cutting the effect of strain hardening is very pronounced.

The material at the tip of the tool, in the deformation zone, undergoes a thermal softening that lowers the hardness of the material, and the strain hardening makes the opposite.

Therefore, it is of fundamental importance to understand at least how incisive the increase of temperature in the process of extrusion cutting is in order to be able to extrapolate a constitutive equation.

However, it is not possible to consider the strain hardening for the difficulty of the argument, in fact, many theories of plastic deformations, as well as the upper

bound model and therefore the theory of extrusion cutting, consider the material perfectly plastic ie with the exponential term of the strain hardening equal to zero.

8.3 Upgrade of the temperature formula in extrusion cutting

Professor De Chiffre [1] had deduced from the theory of the upper bound model that the temperature increase generated by the extrusion was equal to eq. 2.19
The temperature in the deformation zone can be approximated by equation 2.18, assuming an adiabatic temperature increase with the heat resulting from plastic deformation and friction work.
With T_o equal to the initial temperature of the disc which corresponds to the atmospheric temperature ie 20°.
The eq 2.18 would be right only in the case that the extrusion cutting started and ended in a single revolution of the workpiece as the T_o remains constant at 20°.
But this does not happen because ad example, when the disc is new and it is 220mm in diameter, if we make an extrusion of 5 seconds long, with a cutting speed of 100m/min, the disc will take 12 turns. While for a used disc with a diameter of eg 100mm, it will perform 26 revolutions.
So even after the first lap, the temperature of the surface of the disk will be not 20° but it will be a little more, considering that in the previous step it was given heat to the passage of the tool equal to eq. 2.19 minus the heat that the disc has lost to the losses during the time of a turn.
The temperature gradient is towards the inside of the disk, that is towards the material that has not undergone a temperature increase.
The thermal flow always moves from the hot source to the cold source due to the second principle of thermodynamic.
Irradiation losses at these temperature levels are almost nil.
This reasoning would have had almost no sense to exist, if the cooling liquid had been used, which would have absorbed almost all the heat generated, but for reasons of reproducibility and simplification, it was not used.

The starting formula was eq.2.18, the upgrade of formula is:

$$T_i = T_{i-1} + \Delta T - \Delta T_{\text{losses}} \qquad (9.1)$$

Eq. 2.18 can be considered as a constant.

ΔT_{losses} is the difference in temperature generated by the losses that can be convection, conduction and radiation type.

For the above formulas it can be assumed that ΔT_{losses} it is formed only by the conductive contribution, being orders of magnitude higher than the other two.

ΔT_{losses} it depends on the temperature difference between the hot disk surface and the coldest material of disk. We can say also that ΔT_{losses} it is a function of the conductive coefficient "b" typical for each material.

So it can be seen the equation as a function of time and write a first degree differential:

$$\frac{dT}{dt} = \Delta T - \xi T \tag{9.2}$$

with $\xi > 0$ proportionality factor that depends on the material

$$e^{\xi t} \frac{dT}{dt} + \alpha T\, e^{\xi t} = \Delta T\, e^{\xi t} \tag{9.3}$$

That becomes

$$T_{(t)} = e^{-\xi t} \int \Delta T\, e^{\xi t}\, dt \tag{9.4}$$

$$T_{(t)} = \frac{\Delta T}{\alpha} + c\, \Delta T\, e^{-\xi t} \tag{9.5}$$

Now it is possible to find c, putting the time t equal to zero so the T will be the room/workpiece temperature

$$T_{amb} = \frac{\Delta T}{\xi} + c\, \Delta T \tag{9.6}$$

$$c = \frac{T_{amb}}{\Delta T} - \frac{1}{\xi} \tag{9.7}$$

now the final formula:

$$T_{(t)} = \frac{\Delta T}{\xi} + \left(T_{amb} - \frac{\Delta T}{\xi}\right) e^{-\xi t} \qquad (9.8)$$

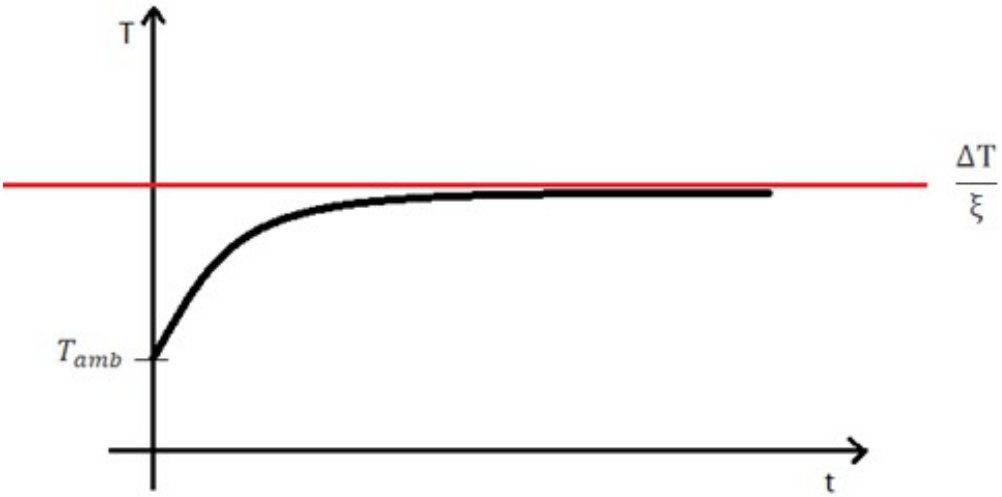

Figure 70: Trend graph equation (9.8)

From the graph (Fig.69) it can be seen that at time zero, ie at the first rotation, the surface temperature of the workpiece is the T_{amb}, then there is a growing exponential that reaches the horizontal asymptote $\frac{\Delta T}{\xi}$.

This means that, in the same conditions, the horizontal asymptote will be as high as the proportional coefficient α will be low, and it depends on the material. It means that the more conductive material is, the faster it will dissipate heat and the horizontal asymptote which represents the temperature reached by the surface of the workpiece will be low and vice versa.

If the material was very little conductive, $\frac{\Delta T}{\xi}$ it could even be higher than $T_{melting}$ and the material on the surface would melt.

A logical question arises:

How soon will It reach the horizontal asymptote?

Or where will be find in the exponential curve in the 5 seconds of extrusion?

It is difficult to answer these questions because α should be obtained experimentally by placing thermocouples on the equidistant disk radius and on the outer circumference a resistance and measuring the speed of the heat flow.

8.4 Thermal simulation

This work was done in ANSYS a finite element simulation program with which a thermal analysis can be done.

A disk has been designed with the features of the workpiece:

Ø=200mm (210mm it would be the new disk)

t=3mm

The characteristics of the material were added, such as density, specific heat and heat transfer coefficient.
A random node was taken on the outer circumference and the 350° thermal source corresponds to it, which will be a point source.
Then the initial temperature of the disk was inserted of 20° and was thermally constrained with it on the opposite surface of the heat source and the simulation was started from zero to 10 seconds.
To understand if the formulations obtained above have a physical validity and not only theoretical, it must be investigated the thermal gradient generated inside the disk, to understand if the temperature remains only on the surface because of the very high speed of passage of the heat source, or it will be entering the disk.

Then it was calculated the time it takes the disk to pass at the equipment of the extrusion cutting of a 200mm disc with a cutting speed of 100m/min
External disk circumference = 0.69m
Cutting speed = 100 m/min = 1.66 m/s

Time of passage on 2 mm of disk $= \frac{0.002}{1.66} = 0.0012$ s

The temperature gradient after 0.0012 s on a pure copper disk with a point heat source of 350° (Fig.70).

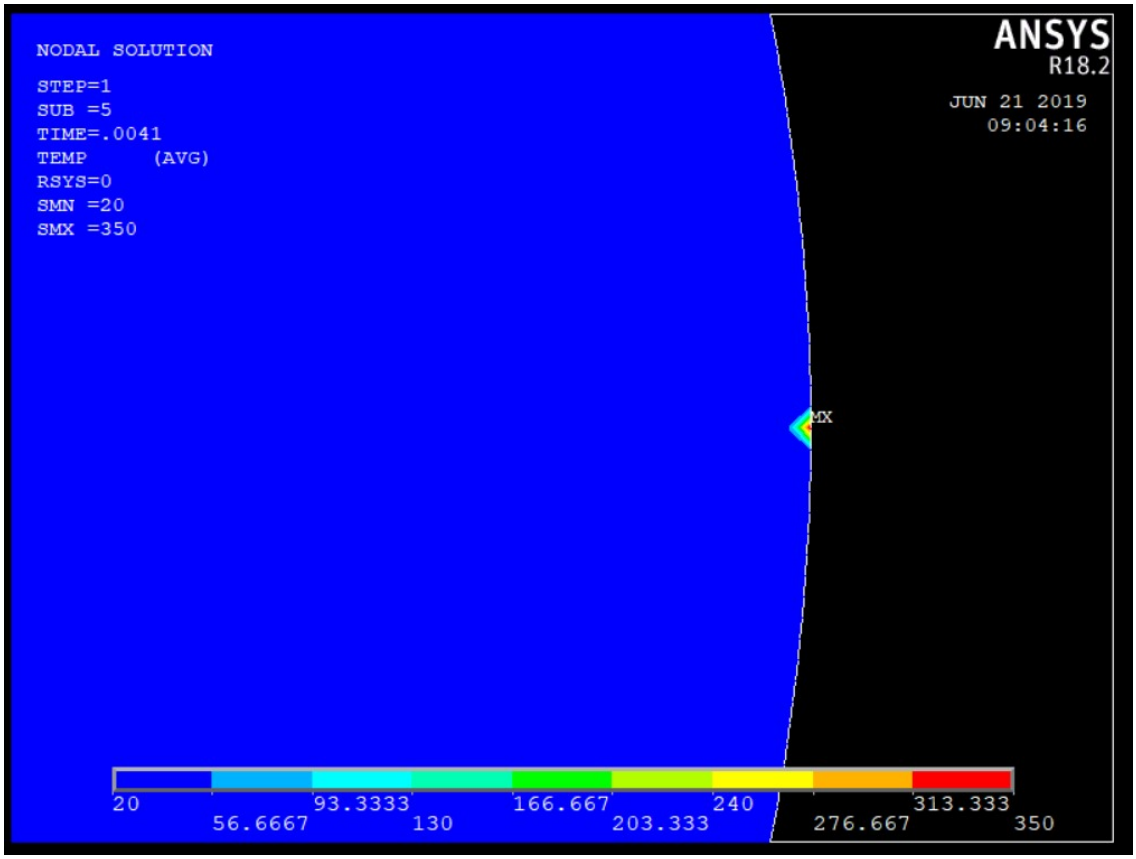

Figure 71: Thermal simlation analysis after one round.

8.5 Temperature conclusion

The simulation shows at which depth and at which speed the heat gradient enters in the workpiece having the same thermal characteristics of the workpiece used in the experiments.

The heat source of 350° at a speed of 100m/min remains on a single point (2mm) about 0.0012 seconds, a time necessary to permit the first millimetres of the surface to achieve the temperature around 200° - 250°. This is due to the characteristics of the material, because copper is an excellent heat conductor.

Obviously the more the disk will have a larger diameter the more time it will pass until the new heat source passes, and therefore the disc will have more time to disperse and spread the heat. It takes exactly 0.41 seconds considering a 200 mm disk, while for a disk that is “consumed”, it means a small diameter, the heat source will pass after shorter time, leaving more heat on the surface.

In conclusion it can be deduced that the starting formula would have had no sense of validity with a large diameter disk and even less sense with a small diameter disk since the temperature remains on the surface having no time to spread.

The reader is reminded that the reasoning is on 0.25mm from the surface, as it is the value of the feed.

However, it remains an unknown factor to evaluate how much the proportional parameter "b" corresponds to each material, referring the question to a future work.

Chapter 9

9 Conclusion

The goal of the project was to conduct an investigation on extrusion cutting as a method to determine the flow stress of metals under the severe conditions experienced during metal cutting. The focus of the project was to see if the obtained results aligned with the analytical model, as this would prove whether or not the model is a viable method for determining flow stress under severe conditions.

The results obtained on brass workpiece with the new equipment fitted well the theorized curve, the stability of the process was very good, the chip obtained was very straight, and shine down to lambda 0.8.

Thus, it is possible to conclude that the extrusion cutting process, as method to obtain the material flow stress on brass, is a robust process. In fact, a huge amount of data in different periods and from different people (i.e. De Chiffre[1], Segalina [3], and Landerghini in this work) were collected, observing a concordance of the obtained results. Therefore, the process can be considered repeatable and reproducible.

On the other hand, the extrusion cutting process applied on copper failed. Indeed, the workpiece keeps having the widening problem, creating difficulties in the data analysis and in the data processing. In fact, the obtained point of minimum is always far from lambda 1.4, even when customized cutting parameters are applied. It is concluded that the way to change the value of rake angle and the cutting speed, is not the correct solution to achieve a process stability.

In the end, the extrusion cutting process has been investigated also with aluminium workpieces, but this material seems to not be extrudable under the nowadays conditions.

Moreover, it has been tried to improve the mathematical model studying the slip line field. Furthermore, a theoretical upgrade of the formula that determines the temperature considering more variables has been developed. Analysing the temperature is significant to define the process of stability because the thermal softening has a relevant influence on the process, since it is not possible to use the

refrigerant. This analysis is also of fundamental importance to be able to derive a constitutive equation of the material.

10 Bibliography

[1] “EXTRUSION-CUTTING” L. De Chiffre 15 January 1976

[2] “EXTRUSION CUTTING OF BRASS STRIPS2 L.De Chiffre 1 November 1982

[3] “Modeling of chip formation”, F. Segalina, Master Thesis 2016

[4] “Investigation on the use of extrusion cutting for material testing”,P. Astrup, Master Thesis 2019

[5] “Material testing of copper by extrusion-cutting”, F. Segalina, L.De Chiffre

[6] “BILL MUNDY THEORY, EFFECTIVE RAKE ANGLE CUTTING TOOLS IN COPPER ALLOYS” *Rev. chil.* 2007, vol.15, n.2, pp.199-203.

[7] “A Guide to Working With Copper and Copper Alloys” antimicrobialcopper.org acesses on 05 March 2019.

[8] J.D. Embury, R.M. Fisher, Acta Metall. 14 (1966) 147–159

[9] G. Langford, M. Cohen, Trans. ASM 62 (1969) 623–638]

[10] Cut-Forming: A New Method of Producing Wire. Hoshi, T. and Shaw, M. (1977). Journal of Engineering for Industry, 99(1), pp.225-228

[11] “Analysis of Large-Strain Extrusion Machining with Different Chip Compression Ratios“ Wen Jun Deng, Ping Lin, Zi Chun Xie, and Qing Li

[12] Large strain deformation and ultra-fine grained materials by machining Srinivasan Swaminathan a, M. Ravi Shankar a, Seongyl Lee a, Jihong Hwang a, Alexander H. King b,∗, Renae F. Kezar a, Balkrishna C. Rao a, Travis L. Brown a, Srinivasan Chandrasekar a, W. Dale Compton a, Kevin P. Trumble b

[13] The Mathematical Theory Of Plasticity (Oxford Classic Texts In The Physical Sciences) by R. Hill 1950

[14] METAL CUTTING PRINCIPLES Second Edition by Milton C. Shaw OXFORD UNIVERSITY PRESS 2005

[15] “Mechanism of continuous equal-channel angular extrusion” V.M.Segal 14 july 2009

[16] Adiabatic Plastic Deformation by Harry C. Rogers 1979

[17]Stelly and Dormeval Shock Waves and High-Strain-Rate Phenomena 1986

[18]J.M.Rodríguez, “Continuous chip formation in metal cutting processes using the Particle Finite Element Method”

[19] https://www.youtube.com/watch?v=yhpWFYagNvc